‘Co-evolution’ of Uranium Concentration and Oxygen Stable Isotope in Phosphate Rocks

Y.Sun[1,2*], W. Amelung[1,2], B. Wu[1], S. Haneklaus[3], M. Maekawa[3], A. Lücke[1], E. Schnug[3], R. Bol[1]

[1]Institute of Bio- and Geosciences: Agrosphere (IBG-3), Forschungszentrum Jülich GmbH, 52425 Jülich, Germany

[2]University of Bonn, Institute of Crop Science and Resource Conservation, Soil Science and Soil Ecology, Nussallee 13, 53115 Bonn, Germany.

[3] Institute for Crop and Soil Science, Julius Kühn-Institut, Federal Research Institute for Cultivated Plants, Bundesallee 69, 38640 Braunschweig, Germany

* Corresponding author (yajie.sun@uni-bonn.de)

Abstract

Phosphate rocks (PRs) used in fertilizer production contain uranium (U), which enters agricultural soils through phosphorus fertilization. However, our knowledge is still limited and cannot explain the different levels of U contamination found in agricultural systems. The paper reviewed the spatial and temporal U variations in PRs to obtain a comprehensive overview of U levels in various PRs worldwide and to investigate why U concentrations in igneous PRs are significantly lower compared to sedimentary PRs, and why less U is present in old sedimentary PRs (Precambrian-Cambrian) than in younger PRs (Ordovician-Neogene). In addition, the natural oxygen isotope compositions of phosphate ($\delta^{18}O_p$) in various PRs were determined to identify their origins in relation to their U concentration. The $\delta^{18}O_p$ values differed among igneous PRs, old sedimentary PRs, and younger sedimentary PRs. Generally, the PRs with low $\delta^{18}O_p$ values had low U concentrations. In igneous PRs, low U concentrations were due to the lack of secondary U enrichment processes after rock formation, with low $\delta^{18}O_p$ values resulting from limited isotope fractionation at high temperature. Conversely, in sedimentary PRs, both U concentrations and $\delta^{18}O_p$ values were influenced by paleoclimate and paleogeographic features. Overall, there is a time-dependent coincidence of processes altering U concentration and $\delta^{18}O_p$ signatures of sedimentary PRs in a similar direction.

Highlights

- The U contents of phosphate rocks (PRs) increased in the order igneous PRs, old sedimentary PRs (Precambrian-Cambrian), younger sedimentary PRs (Ordovician-Neogene).
- The values of $\delta^{18}O_p$ of PRs increase as follows: igneous PRs, old sedimentary PRs (Precambrian-Cambrian), younger sedimentary PRs (Ordovician-Neogene).
- In sedimentary PRs, there is a time-dependent coincidence of processes altering U concentration and $\delta^{18}O_p$ signatures in a similar direction.

Keywords: phosphate rocks; $\delta^{18}O_p$; uranium; U/P_2O_5

1. Introduction

Phosphorus (P) is a vital nutrient and energy carrier for life and it is thus also an indispensable fertilizer in agriculture including animal husbandry. The main route for the P supply relies on the exploitation of geological phosphate deposits, the availability of which is likely limited to the next 40 to 400 years (Obersteiner et al., 2013). However, phosphate rocks (PRs) also contain a significant amount of uranium (U) (0.3 to 247 mg U kg^{-1}), with typical average concentrations of 75 to 120 mg kg^{-1} (Altschuler, 1980).

Most recently Windmann (2019) reported an average geometric mean in 128 sedimentary phosphate rock of 56.9 mg U kg^{-1}, compared to only 7.56 mg U kg^{-1} in 22 rocks of igneous origin. Therefore, mineral P fertilizers produced by PRs may also contain various amount of U which can be added to agricultural soils through the application of mineral P fertilizers (Schnug and Haneklaus, 2015). Depending on the source and the amounts of mineral P fertilizers applied, different levels of U accumulation have been observed in agricultural soils in various countries (e.g. Rothbaum et al., 1979; Bigalke et al., 2018).

To avoid potential U contamination and explain the different levels of U accumulation in agricultural soil, it is necessary to reveal the variations of U concentrations in PRs from different deposits. Furthermore, geochemical signatures of PRs are needed to identify the origins of PRs. How and why U concentrations are related to the origin of PRs are the key questions to be understood. Previous studies revealed that, at present, no single element concentration can be used to differentiate PR deposits (Sattouf et al., 2007). An alternative way is to identify the origin of deposits of PRs by using stable isotopes, such as strontium (Sr) isotopes (Sattouf, 2007). For instance, Sattouf et al. (2007) used ^{87}Sr/^{86}Sr isotope ratios to classify PRs into four different groups: 1) igneous rock phosphates from Russia (Kola), sedimentary rock from: 2) Algeria, Israel, Morocco, Tunisia and Syria, 3) the USA, and 4) Senegal and Togo. In addition, ^{234}U/^{238}U ratios can be used to distinguish PRs and P fertilizers originating from the USA and those of other regions (Sattouf et al., 2008).

Taking advantage of stable isotope discrimination processes to identify the origin of PRs does not apply for P, because this element does not have different stable isotopes. However, we may take advantage of natural oxygen (O) isotope compositions of phosphate ($\delta^{18}O_p$) in the PRs. $\delta^{18}O_p$ is selected as a potential indicator of the origin of the phosphate due to the fact that O stable isotope signatures may provide unique information on the paleo-environmental conditions during PRs formation. Based on pioneering research by Longinelli and Nuti (1973), who constructed an empirical equation between inorganic P-water oxygen isotope fractionations and temperature,

$$\mathrm{T} = 111.4 - 4.3\left(\delta^{18}\mathrm{O}_{\mathrm{p}} - \delta^{18}\mathrm{O}_{\mathrm{w}}\right)$$

where T is the average environmental temperature, $\delta^{18}O_p$ is the natural oxygen isotope composition of phosphate and $\delta^{18}O_w$ is that of water. Oxygen in phosphate is bound tightly to P such that isotope exchange of O between phosphate and surrounding water is essentially negligible by abiotic processes even over geological time scales at low temperatures which relevant to earth surface environments (Jaisi and Blake, 2014; Longinelli and Nuti, 1973; Lecuyer et al., 1999; Blake et al., 2010; Shemesh et al., 1983). This is true even at exterme pH values (10 M nitric acid and 14 M NH_4OH) and at high temperature condition(70 ^{o}C), which has been proved on laboratory time scales (Blake et al., 2010). However, using the $\delta^{18}O_p$ value as a tracer for different PR deposits in relation to the occurrence of U is still pending. We therefore aimed to look for possible indicators that can relate the origin of PRs to their U and P content.

This study was performed to contribute to a better background understanding why agricultural soils may show different levels of U contamination through P fertilization. The first part of the paper provides an overview of the spatial and temporal distributions of U in PRs, the second investigates the degree to which the $\delta^{18}O_p$ values of PRs can reflect their deposition, and the third presents the correlation between the U concentration and the natural $\delta^{18}O_p$ for different PR deposits. Details on U geochemistry in PRs and other related isotope studies are not re-reviewed here, since this has already been undertaken by several authors, e.g. Jarvis (1995), or Kolodny and Luz (1992).

2. Materials and Methods

Data collection

Published U concentrations from overall 18 igneous and 277 sedimentary deposits were retrieved from the literatures. To supplement this data, we collected 74 sedimentary PRs from 11 countries: Algeria, Brazil, China, Israel, Morocco, Russia, Senegal, South Africa, Syria, Togo, USA, and 9 igneous PRs from Brazil, China, South Africa and Russia. All these PRs samples were analyzed for total U concentration and oxygen isotope composition in phosphate ($\delta^{18}O_p$).

Uranium analyses

Total concentrations of U in PRs were analyzed by inductively coupled plasma spectrometry (ICP-MS, Thermo Fisher Scientific, Bremen, Germany) after the digestion of 0.05 g soil with 0.25 g lithium meta/tetraborate at 1050 ^{o}C for 3 h. The analytical error for total concentration measurement by ICP-MS was within 2%.

$\delta^{18}O_p$ analyses

One gram of each ground phosphate rock samples was shaken with 50 ml 1M HCl for 16 hours. The soil-acid mixture was then centrifuged for 15 minutes at 1300 g and filtered through Whatman GF/F filters. The supernatant was then used for phosphate purification. The purification procedures followed Tamburini et al. (2010). This method is based on the preparation of ammonium phosphomolybdate salts (APM), which are precipitated by adding ammonium nitrate solution and ammonium molybdate to the sample solution. Subsequently, the APM was dissolved again in citric acid solution and Mg added to produce a magnesium ammonium phosphate mineral precipitate (MAP). The precipitation products were then dissolved with 0.5 mol l^{-1} nitric acid and purified via a DOWEX® 50 WX8 (200 -400 mesh) cation resin. By adding Ag nitrate solution, the phosphates to be analyzed were precipitated as silver phosphate (Ag_3PO_4). The $\delta^{18}O_p$ values were finally determined by high temperature reduction of Ag_3PO_4 to CO by a high-temperature conversion isotope ratio mass spectrometry (HTC-IRMS) system, composed of a high temperature oven (HEKA tech GmbH, Germany) and the IRMS Isoprime (Elementar Analysensysteme GmbH, Germany). All measurements were performed together with four in house laboratory Ag_3PO_4 standards spanning as $\delta^{18}O$ range between 2.2‰ and 33.7‰ Vienna Standard Mean Ocean Water (VSMOW). In house standards were calibrated against two International Atomic Energy Agency (IAEA) benzoic acid standards, IAEA 601 ($\delta^{18}O$= 23.1‰ VSMOW) and IAEA 602 ($\delta^{18}O$= 71.3‰ VSMOW). All measured $\delta^{18}O_p$ values are reported normalized to the VSMOW scale. Analytical uncertainty calculated on replicate analysis of in house standards was better than ± 0.25‰.

Details of U concentration and oxygen isotope signatures of the different PRs can be found in the supplementary material S1-3.

3. Results and Discussion

3.1 Spatial and temporal distributions of uranium concentrations in phosphate rocks

3.1.1 Spatial distribution

The main phosphate ores types include marine sediments, igneous rocks and guano. About 75% of the world’s phosphate resources are obtained from sedimentary PRs, whereas 15-20% are obtained from igneous deposits (Pufahl and Groat, 2016; Petr, 2016). Guano, i.e., mainly deposits from birds, penguins, cormorants and bats, is enriched in P but is not available in sufficient quantities for global use (Pufahl and Groat, 2016). The majority of sedimentary phosphate deposits have been formed under marine conditions (e.g. Nathan, 2012) and are quantitatively the most important source of the world's phosphate rocks for fertilizer production (U.S. Geological Survey, 2018). Sedimentary phosphate deposits are found on almost every continent, in North Africa and the Middle East, China, and the United States and range in age from Precambrian to Recent (e.g. Cook, 1984) (Fig. 1). The largest P reserves are found in the Late Cretaceous-Eocene South Tethyan phosphogenic province, hosting 85% of the world's PR reservoir (Cook, 1984).

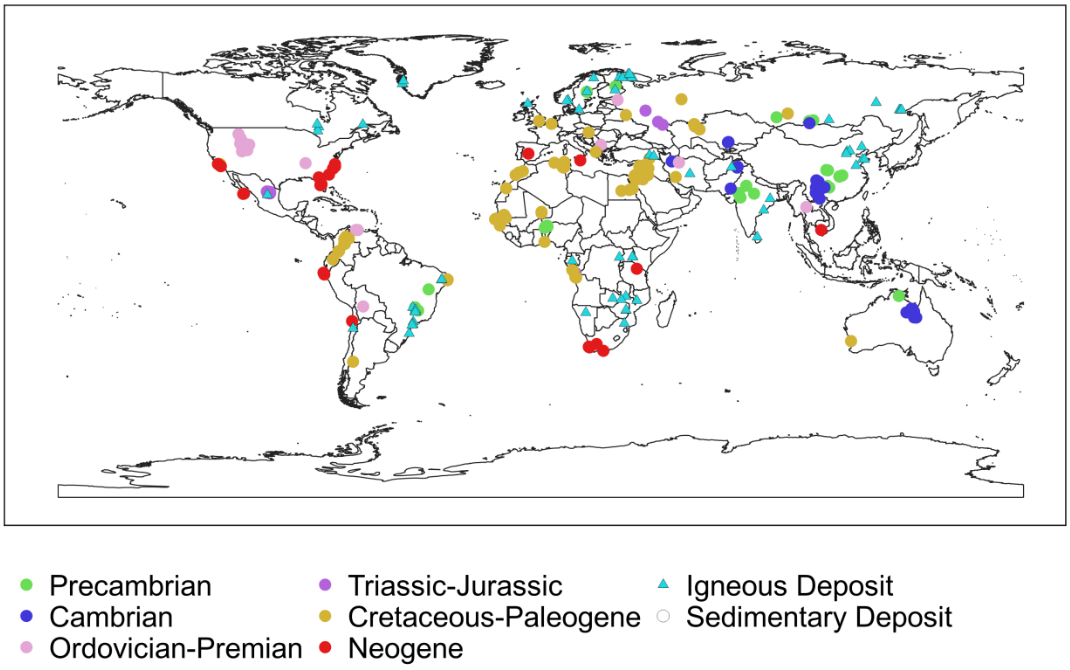

Figure 1. Distribution of sedimentary and igneous phosphate deposits with respective ages. (Age is the considering factor only for sedimentary PRs. Data source for sedimentary and igneous phosphate deposits: Chernoff and Orris, 2002.)

Igneous phosphates are a type of magmatic rock in which the element P was incorporated into the crystal structure of apatite, which took place when the mineral crystallized from the cooling melt (Pufahl and Groat, 2016). In general, the spatial and temporal distributions of igneous apatite deposits are similar to those of alkaline igneous rocks. Igneous phosphate deposits are also geographically fairly widespread and range in age from Precambrian to Tertiary (Cook, 1984). The typical grade of P_2O_5 is 5-15 wt % and most associated phosphate deposits are small and not suitable for commercial exploitation (Pufahl and Groat, 2016). The world's largest source of igneous PRs stems from the Devonian Khibiny Alkaline Complex in Russia's Kola Peninsula, contributing more than 50% of global igneous PRs use (Van Kauwenbergh et al., 2010). The Jacupiranga deposits of Brazil, located at the edges of Paleozoic basins and the Paleoproterozoic Palabora Complex deposit in South Africa, are the two largest reserves of igneous PRs (Van Kauwenbergh et al., 2010; Pufahl and Groat, 2016).

The PRs from different countries generally show various degrees of enrichment with U (Fig. 2). The data compilation reveals that igneous PRs, originating, for instance, from Russia, China, South Africa and Finland, generally display U concentrations in the range of 0.3-64 mg kg^{-1}, i.e. much lower than sedimentary PRs (0.6-390 mg kg^{-1}). Among the examined sedimentary PRs, about 60% exhibited U concentrations from 80 to 150 mg kg^{-1}. Sedimentary PRs from Morocco, USA and Israel usually showed relatively high U concentrations, with medians of 94, 116 and 129 mg kg^{-1}, respectively, and also wide content range of 3-250, 57-245 and 8-215 mg kg^{-1}, respectively. However, some sedimentary phosphate rock samples from Australia, Saudi Arabia, and Turkey only contained U in concentrations in the range of 20-50 mg kg^{-1}. In particular, the PRs originating from China show lower U concentrations in the range of 2.0 to 31 mg kg^{-1} with a median of 11.4 mg kg^{-1}. According to this data base, PRs from selected countries appear to exhibit a lower probability for U contamination than from other countries; yet the range is large and U concentration alone cannot be used to differentiate the origin of the different PRs.

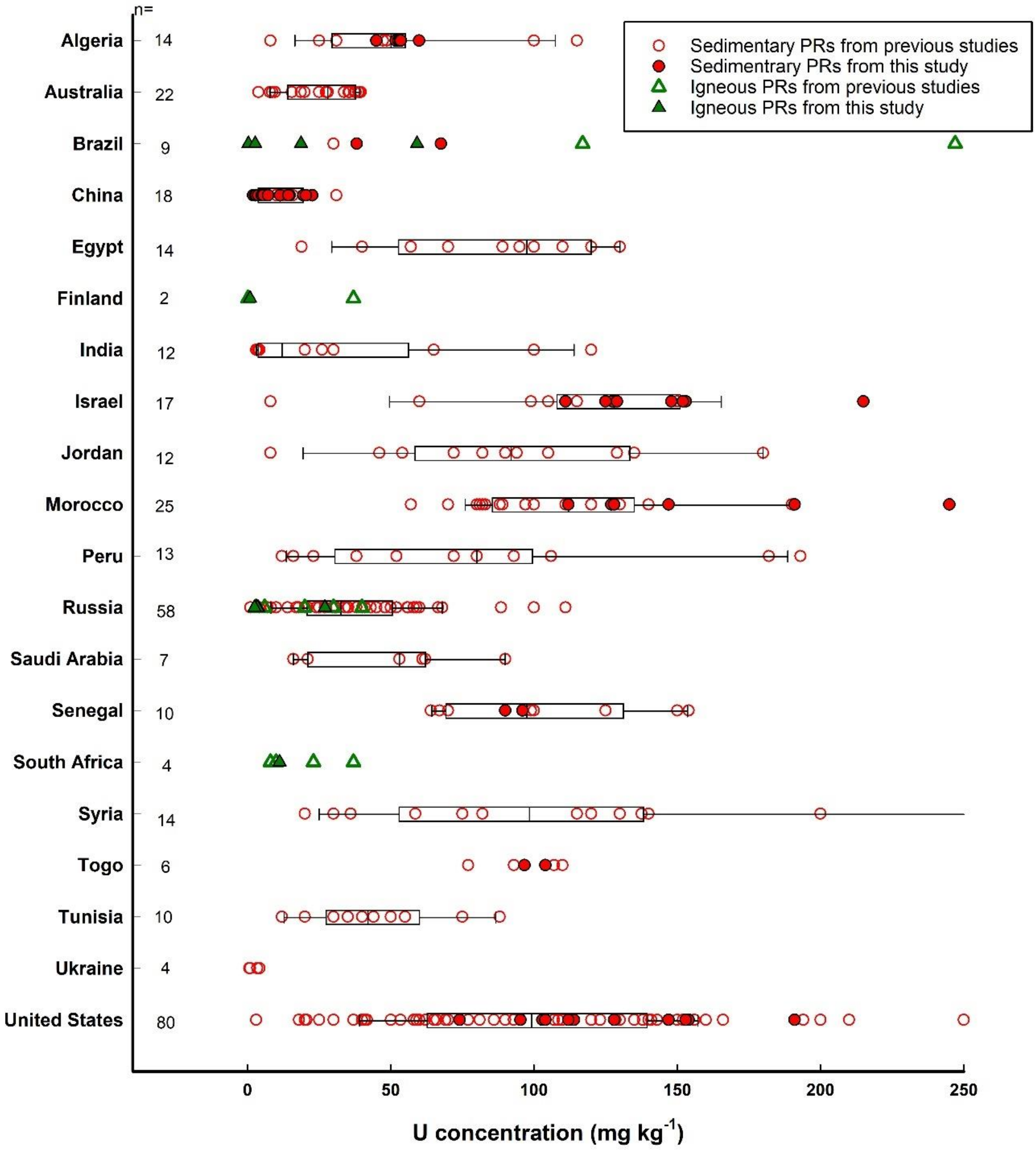

Figure 2. Combination of scatter diagram and boxplot for U concentrations in phosphate rocks (PRs) from 20 countries. (Data include a total of 22 igneous and 339 sedimentary samples. Data sources: Altschuler et al., 1958; Altschuler et al., 1980; Banerjee et al., 1982; Baturin and Kochenov, 2001; Cevik et al., 2010; Cook et al., 1990; Cook, 1972; Dissanayake and Chandrajith, 2009; Dar et al., 2014; Hayumbu et al., 1995; Howard and Hough, 1979; Jallad et al., 1989; Khater et al., 2016; Levina et al., 1976; Makarov, 1963; Menzel, 1968; Pantelica et al., 1997; Parker, 1984; Pokryshkin, 1981;Sattouf, 2007; Schnug et al., 1996; Syers et al., 1986; Wakefield, 1980; Van Kauwenbergh, 1997; Zanin et al., 2000.)

3.1.2 Temporal distribution

In this study, the U content was normalized to the P_2O_5 content (as U/P_2O_5), in order to take into consideration of the fact that U in PRs is generally associated with the phosphoric phase (Brookfield et al., 2009; Föllmi, 1996; Lucas and Abbas, 1989). Overall, the ratios of U/P_2O_5 in sedimentary PRs range from 0.02 to 17.7 in deposits of all different ages, which shows that U deposition is highly variable with respect to phosphorus content (Fig. 3). The median values of U/P_2O_5 of the PRs in each age period decline in the deposits with increasing geological age of the deposits, with median values of 0.1 for Precambrian PRs, 1.2 for Cambrian PRs, 2.9 for Ordovician-Permian PRs, 2.6 for Triassic-Paleogene PRs and 3.5 for Neogene PRs, respectively. The distributions of U/P_2O_5 in PRs of Ordovician-Permian, Triassic-Paleogene and Neogene age are rather similar. In contrast, most Precambrian and Cambrian PRs analyzed so far exhibit low U/P_2O_5 ratios below two. Obviously, the very ancient PRs are characterized by low U/P_2O_5 ratios. A few previous studies also noticed the U-depletion in ancient sedimentary PRs (Sokolov, 1996; Volkov, 1994). However, the reasons for U depletion in ancient PRs were seldom investigated. In the following sections the focus in on exploring the mechanisms for U deposit in PRs.

3.2 Mechanisms of various deposition processes of U in phosphate rocks

3.2.1 U speciation in PRs

Apatite is the most abundant phosphate mineral. It is believed that U is mainly associated with apatite as radioactivity detected in phosphate nodules mostly originates from apatite. In addition, U contents extracted from various PRs samples are essentially the same when only apatite or apatite plus silicates is dissolved (Altschuler, 1958). Igneous apatite rocks consist of three primary mineral forms: chlorapatite [$Ca_5(PO_4)_3Cl$], hydroxylapatite [$Ca_5(PO_4)_3OH$], and fluorapatite [$Ca_5(PO_4)_3F$] (Jarvis, 1995). In sedimentary apatites, the main ore mineral is francolite

$[Ca_{10-a-b}Na_aMg_b(PO_4)_{6-x}(CO_3)_{x-y-z}(CO_3\cdot F)_{x-y-z}(SO_4)_zF_2]$ (Jarvis, 1995; Petr, 2016). Two states of U can be present in these PRs either as UO_2, UF_4 or $Ca(UO_2)_2(PO_4)_28H_2O$ phases, or as isolated U^{4+} ions or UO_2^{2+} radicals adsorbed on mineral surfaces or within internal discontinuities (Hendricks and Hill, 1950). It may also be substituted structurally in apatite, as U^{4+} by replacement of Ca^{2+}, owing to the virtually identical ionic radii of U^{4+} (1.05Å) and Ca^{2+}(1.06Å) (Baturin and Kochenov et al., 2000). Uranium in the structure of apatite dominates as U (IV). The present of U (VI) fixed as a surface-coordinated uranyl pyrophosphate is derived largely from post-depositional oxidation of U(IV) (Altschuler, 1958). In addition, the studies on submarine phosphorite also indicate the observed U(VI) content are not solely the product of surface oxidation and that U is probably incorporated in apatite in both oxidation state (Kolodny and Kaplan, 1970; Burnett and Veeh, 1977).

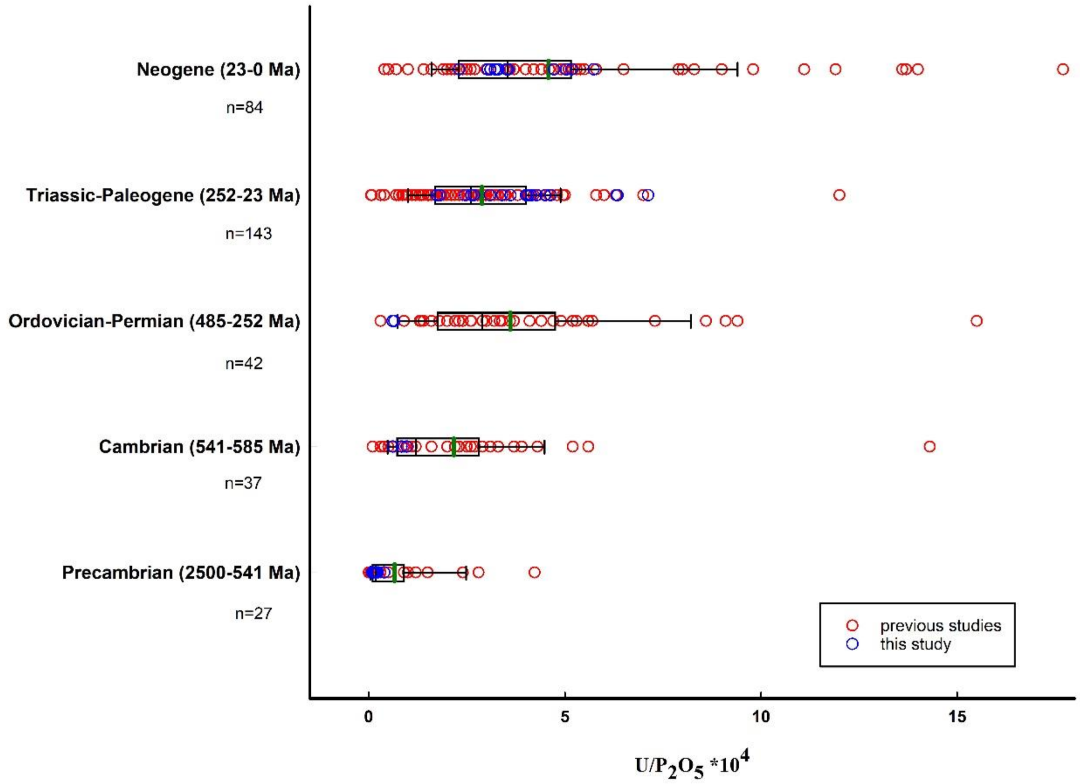

Figure 3. Distribution of U/P_2O_5 in sedimentary PRs during geologic time from Precambrian to Holocene. The plot is a combination of scatter diagram and boxplot. The green lines are mean values for each period of geologic time.

3.2.2 Variation of U deposition in igneous and sedimentary PRs

Differences in U/P_2O_5 ratios reflect to a large degree the diversities in the formation mechanisms for igneous and sedimentary PRs. Apatite deposits of igneous origin occur as intrusive masses or sheets, as hydrothermal veins or disseminated replacements, or as marginal differentiations along or near the boundaries of intrusions, or as pegmatites (McKelvey, 1967). It has been reported that most igneous apatites contain U concentration between 40-80 mg kg^{-1} (Altschuler et al., 1958). Most recently Windmann (2019) reports from a much larger sample population a geometric mean of 7.56 mg kg^{-1} with a variation coefficient of 119%. The amount of U available to apatite largely depends on special environmental circumstances, presumably, the production of U (IV). The occurrence of U in igneous apatite is governed by the equilibrium conditions prevailing in the magma during the precipitation of apatite (Altschuler et al., 1958). The amount of U available to igneous apatite is regulated by apatite's capacity, as well as the capacities of the other hosts coextensive with U and thus reflects the total equilibrium in the magma (Altschuler et al., 1958). In contrast to igneous apatite, the occurrence of U in marine sedimentary apatite is not governed solely by the equilibrium condition in the ocean, but also by the subsequent secondary enrichment processes during marine reworking (Baturin and Kochenov, 2001; Altschuler et al., 1958). The enrichment of U in sedimentary apatite implies that apatite has acquired and sequestered additional U from the sea water. Uranium is removed from the seawater by diffusion across the sediment-water interface. Dissolved U is drawn into the anoxic zone of sediment layer along a concentration gradient caused by the precipitation of U(VI) to U(IV). This transformation is induced by microbially mediated dissolution of manganese and iron oxides, and sulfate reduction (Klinkhammer and Palmer, 1991; Soudry et al., 2002). The presence of apatite can actively affect the course of the reduction reactions ($(UO_2)^{+2}$ + reductant ↔ U^{+4} + oxidized reductant), by sequestering U (IV), thereby a continuous supply of U(IV) (Altschuler et al., 1958).

3.2.3 Mechanism of U variation in sedimentary PRs

Even if U is enriched in sedimentary PRs, the reasons for considerable low U concentrations in ancient PRs are complex. They may be a comprehensive result of three factors: i) the evolution of U in the earth during geological history, ii) different paleogeographic features, and iii) weathering and catagenesis, which all affect the fate of U in phosphate deposits, as outlined below.

Geochemical evolution of U along the geologic units

The U concentration in sediments reflects the size of the local and perhaps global marine environment U reservoir (Partin et al., 2013). The geochemical evolution of U in marine is affected by two major events: the development of an oxygenated atmosphere about 2.2 billion years ago and the development of land plants at about 0.4 billion years ago (Cuney, 2010). Before oxygenation started, the reduced conditions in the absence of O, resulted in low solubility and low concentration of U in water (Partin et al., 2013). The lack of U enrichment in ancient PRs deposits in this study confirms the low concentration of soluble U in marine waters. In the period of 2.3-0.45 Ga, during and after the Great Oxidation Event (GOE) when oxygen increased near to the present atmospheric level, oxidative processes took place in terrestrial environments and the continental fluxes of dissolved U to the oceans increased dramatically (Holland, 1984). The last period was from 0.45 Ga to the present, when the Earth was colonized by plants. Uraninite and coffinite were precipitated from the U-rich near-surface waters into the oxygenated and organic-rich continental sediments; thus, total U concentrations in the sediments increased significantly (Cuney, 2010). As a consequence, higher U concentrations were found in younger PRs.

Paleogeographic features

The U depletion in ancient phosphorites was additionally caused by the paleogeographic features of relevant basins (such as in Asia and Africa), where U influx was considerably less pronounced during the phosphorus influx into the phosphate accumulation zones (Stephens and Carroll, 1999; Baturin and Kochenov, 2001). In contrast, the U-enrichment in later geologic time units was associated with paleogeographic reconstructions upon upwelling, which promoted both U and P deliveries into the shallow shelves (Baturin and Kochenov, 2001). Additionally, the process of U accumulation is believed to be related to sedimentary reducing conditions (Avital et al., 1983; Altschuler, 1958), where soluble U(VI) was reduced to insoluble U(IV) and deposited in the sediments. Elevated loads of organic matter led to reduced sedimentary conditions (McManus et al., 2005) turning them into a significant sink for U (Altschuler, 1958).

Weathering and catagenesis

Apart from the geochemical conditions during U influx and accumulation, weathering and catagenesis can control the residence time of U within the reservoir (Zanin et al., 2000). The effects of subaerial weathering remove apatite constituents from the apatite structure. Consequently, apatite decomposes, and soluble mineral phases and speciation of trace elements, such as U, are lost during weathering (Howard and Hough 1979; Zanin et al., 1985). In addition, the composition and texture of sedimentary apatite could be essentially modified in catagenesis (Zanin et al., 1985). The catagenesis processes correspond to remove isomorphic impurities from carbonate-apatite, such as carbonate ions, isomorphic trace elements (e.g. Sr, Cd, U), sodium, and H_2O^+ (Zanin et al., 1985). Therefore, the U concentrations in ancient PRs are relatively low, since the ancient phosphate rocks were exposed to catagenesis for a longer period (Baturin and Kochenov, 2001).

3.3 Oxygen isotope signature in phosphate deposits

As all the processes mentioned so far interact with each other, with unclear relations to the origins of phosphates in PRs, the oxygen isotope natural abundances of phosphates ($\delta^{18}O_p$) is included as an additional indicator to distinguish PRs of different origins and with different U concentrations.

3.3.1 Oxygen isotope fingerprint of phosphate rocks of various origins

The O isotope compositions of the phosphates in the PRs are variable, thus fingerprinting their deposits (Fig. 4). In general, three different groups of PRs differing in their $\delta^{18}O_p$ natural abundance values can be differentiated: 1) igneous PRs from Brazil, China, Russia and South Africa ($\delta^{18}O_p \leq 8.8$ ‰), 2) sedimentary PRs from China and Brazil ($\delta^{18}O_p$ 12.2 -18.2 ‰), and 3) sedimentary PRs from Algeria, Israel, Morocco, Russia, Senegal, South Africa, Syria, Togo and the USA ($\delta^{18}O_p \geq 18.8$ ‰; Fig. 4).

.

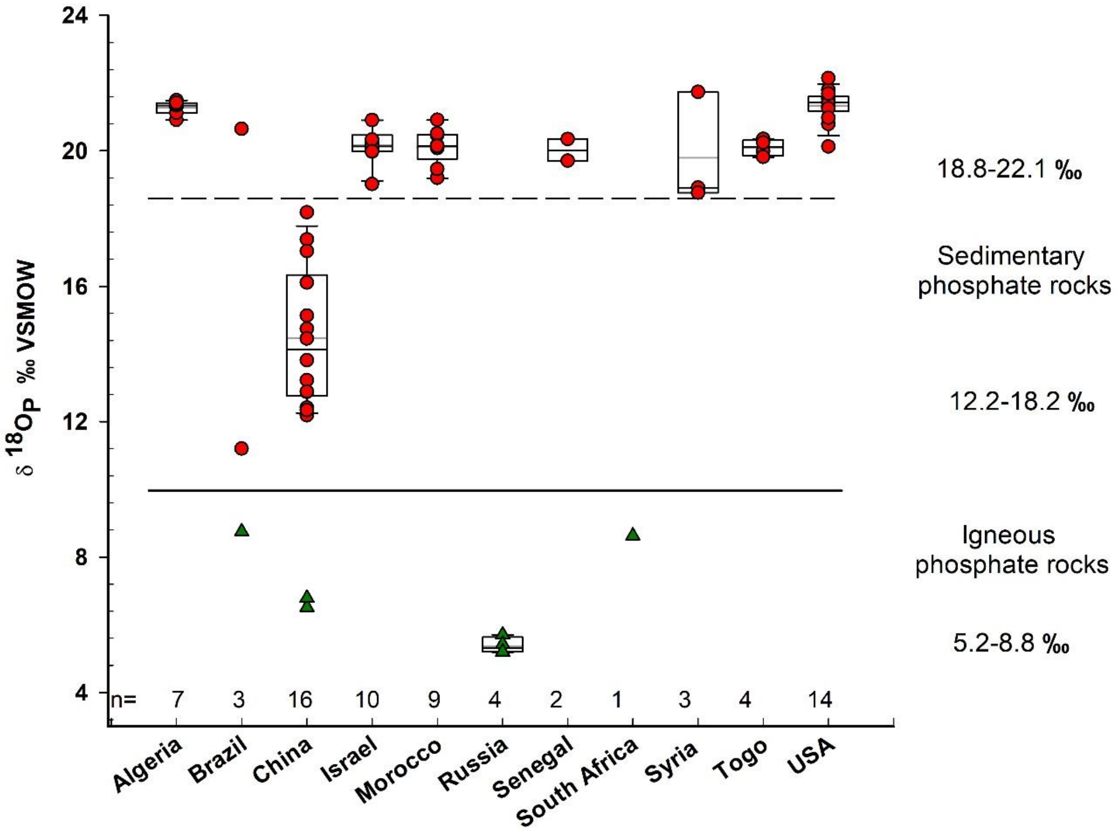

Figure 4. Variation of oxygen isotope composition ($\delta^{18}O_p$) in phosphate rocks (PRs) from different countries.

All igneous PRs show relatively low $\delta^{18}O_p$ values (5.2 - 8.8‰), which are comparable in magnitude with the $\delta^{18}O_p$ values of igneous apatite reported previously (Taylor, 1962). In contrast, larger and a wider range of $\delta^{18}O_p$ values (from 12.2 to 22.1‰) are found in sedimentary PRs. Notably, the $\delta^{18}O_p$ values of sedimentary PRs from China, as well as one sample from Brazil, show an intermediate range of $\delta^{18}O_p$ values (12.2-18.2‰). The other sedimentary PRs of this study exhibit a considerable narrow range of $\delta^{18}O_p$ from 18.8 to 22.1‰.

3.3.2 Mechanisms causing various $\delta^{18}O_p$ in phosphate rocks

The final $\delta^{18}O_p$ isotope composition in PRs largely depends on that of the source water and the $\delta^{18}O_p$ values within these rocks may be then regarded as reflections of their crystallization history (Taylor, 1962). Potential sources of fluids involved in the formation or alteration of phosphate deposits include magmatic water, meteoric water and ocean water. These three are characterized by specific $\delta^{18}O_w$ values. Magmatic water which has never been in contact with the hydrosphere has $\delta^{18}O_w$ values from 5 to 8 ‰ (Shepherd et al., 1985). The relatively low $\delta^{18}O_p$ values of igneous PRs in this study are close to these low $\delta^{18}O_w$ values of magmatic water (Kusakabe and Matsubaya, 1986). In addition, limited fractionation will take place in the high temperature magma during the precipitation of the apatite. Therefore, apatite in igneous rocks may retain the same low $\delta^{18}O$ as the magmatic water. The variation of $\delta^{18}O_p$ values in igneous PRs reflects the range of temperatures at which the fluids were produced.

The $\delta^{18}O_p$ values of sedimentary PRs in this study are in the range of marine sedimentary phosphate (9.2-23.9‰) as reported previously by Shemesh et al. (1988). The ultimate fluid origin of sedimentary materials involves trapped seawater, or evolved meteoric water (Fayek, et al., 2011). The details of $\delta^{18}O$ in seawater will be discussed in the following. Meteoric waters, in turn, are abundant in rivers, lakes, glaciers and groundwater. They usually exhibit elevated $\delta^{18}O$ values due to various degrees of water-rock interactions (Shepherd et al., 1985). In addition, the geographic (such as island effect) (Tang et al., 1998) and climatic parameters (e.g. latitude, elevation, distance from the coast) correlated with the $\delta^{18}O_p$ values (Dutton et al., 2005). These different influences thus explain the large variations in O isotopic compositions, as well as the variations of $\delta^{18}O_p$ values in most of the analyzed sedimentary PRs.

The reasons for the variation of lower $\delta^{18}O_p$ values in sedimentary PRs also deserve to be considered. It can be noted that low $\delta^{18}O_p$ values of the sedimentary PRs were accompanied by older ages of formation. For instance, the sedimentary PRs from China which formed in Ediacaran-Cambrian (485-635 Ma) and Devonian (359-419 Ma) periods (Cook and Shergold, 2005; He and Zhou, 2015), have lower $\delta^{18}O_p$ values. Younger sedimentary PRs from Algeria, Israel, Morocco, Senegal, South Africa, Syria and Togo, formed in Cretaceous-Paleogene (56-145 Ma) times (Notholt, 1986), on the other hand, exhibited relatively higher $\delta^{18}O_p$ values in the range of 18.7-21.4‰. The youngest PRs in this study were from the USA, and also exhibited the highest $\delta^{18}O_p$ values, although within a narrow range (20.1-21.8‰; Fig. 4). The findings indicate that there is a clear relation between the $\delta^{18}O_p$ values and the age of the sedimentary PRs. This conclusion is supported by earlier suggestions of, e.g. Longinelli and Nuti (1968), and Shemesh et al. (1988), who found that $\delta^{18}O_p$ values decreased sharply from recent to Cretaceous times (66-145 Ma), and decreased further with a gentle slope to the Precambrian (541 Ma) (Fig. 5). The underlying mechanisms, however, are still a matter of debate, particularly because there is no consensus yet to whether it was temperature or the $\delta^{18}O$ value of the ancient ocean water that led to low $\delta^{18}O_p$ values in ancient rocks (Blake et al., 2010; Longinelli and Nuti, 1968; Shemesh et al., 1983, 1988). Three main explanations have been offered: 1) ocean water temperatures must have decreased from ancient to recent times (Knauth and Epstein, 1976; Knauth and Lowe, 2003; Shemesh et al., 1983), 2) the changing $\delta^{18}O$ value of sea water over time (e.g. Chase and Perry, 1972), 3) increasing $\delta^{18}O_p$ values from ancient to recent times caused by post-depositional alterations (Shemesh et al., 1983).

The opinion that ancient PRs were deposited under high temperatures has been put forward by many studies (Shemesh et al., 1983; Piper and Kolodny, 1987; Blake et al., 2010). Such higher temperatures could have been either a reflection of global phenomena, i.e. of warmer oceans in the geological past, or of a shift in the site of phosphate rocks formation in the ocean (Kolodny and Luz, 1992). Assuming that the $\delta^{18}O_w$ of the sea water was about 0 ‰ and that this value was maintained over geologic timescales in the absence of glacial periods (Muehlenbachs, 1998), the sedimentary

PRs should thus have formed at an isotopic equilibrium with $\delta^{18}O_w$= 0‰. The calculated ocean temperatures of the Ediacaran-Cambrian (485-635 Ma), Devonian (359-419 Ma), Cretaceous-Paleogene (56-145 Ma), and Neogene-Quaternary (0.01-23 Ma) in this study would then have been 42.2 ^{o}C, 36.7 ^{o}C, 23.9 ^{o}C and 19.6 ^{o}C, respectively. This indicates that the temperature of the ocean slowly decreased with time and the evolution of the Earth. An even higher temperature (> 60 ^{o}C) has been proposed for Archean and early Proterozoic waters (Knauth and Epstein, 1976; Robert and Chaussidon, 2006).

The $\delta^{18}O_w$ values of the ocean can only change very slowly, since the residence time of water in the ocean is very long compared to hydrothermal circulation (Land and Lynch, 1996), and rates of chemical weathering on the continents are also slow. Hence, the seawater $\delta^{18}O_w$ value is assumed to have been fairly constant over time, buffered by hydrothermal and weathering processes at mid-ocean ridges to a $\delta^{18}O_w$ value of about 0‰ (Standard Mean Ocean Water, SMOW) (e.g. Muehlenbachs, 1998; Holland, 1984). Hren et al. (2009) disagreed with this view and considered that, the $\delta^{18}O_w$ value could have been as low as -10 to -13‰ in the Archaean ocean with a subsequent increase to present-day values. However, Blake et al. (2010) argued that based on the equation of Longinelli and Nuti (1973) mentioned above, such a conclusion would imply that the $\delta^{18}O_p$ values of Archaean marine phosphate would have been formed at an unrealistic ocean temperature of -8 ^{o}C to -30 ^{o}C. This conclusion favored the former interpretation that the increase of $\delta^{18}O_p$ with decreasing geological age of the PRs most likely reflects the progressive cooling of sea temperatures during Earth's history. In any case, there was a coincidental 'co-evolution' (but not coupled) of $\delta^{18}O_p$ signature in PRs and their U concentration, as a function of sedimentary PRs' age.

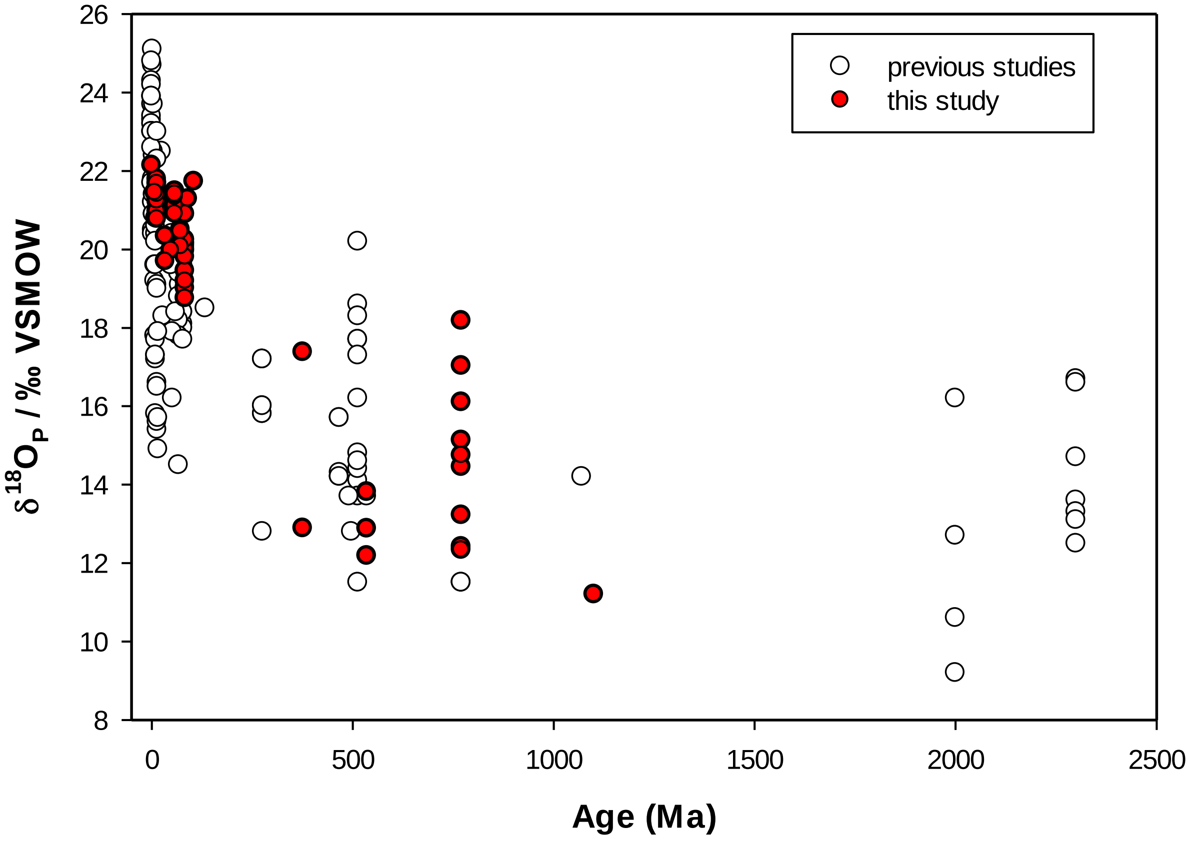

Figure 5. Oxygen isotope in phosphates ($\delta^{18}O_p$) as related to the geological age of the sedimentary phosphate rocks (Data for circles are from Shemesh et al., 1983, 1988 and data for red points are from this study).

It should be noted that despite a likely wholescale lowering of $\delta^{18}O_p$ values in older marine PRs, the ranges of $\delta^{18}O_p$ values found for the PRs in this study are broad, even for those originating from a given geographic region and geologic time unit. It seems therefore likely that additional effects by post-depositional isotopic exchange altered the $\delta^{18}O_p$ value between the O in phosphate and that in the surrounding water. Earlier work by Longinelli and Nuti (1968) proposed that post-depositional processes could have shifted the $\delta^{18}O_p$ values of sedimentary rocks to lower levels, since alteration commonly occurred in the presence of ^{18}O-depleted meteoric waters or at elevated temperature (Jaffres et al., 2007). Moreover, $\delta^{18}O_p$ studies of fish debris, pointed to considerably larger values than in associated phosphate rocks, indicating the possible existence of a significant post-depositional isotopic exchange in the latter (Kastner et al., 1990).

3.4. Relationship between the U/P_2O_5 and $\delta^{18}O_p$ in phosphate rocks

The U/P_2O_5 and $\delta^{18}O_p$ values showed a clearly positive correlation (Fig. 6), pointing to some kind of 'co-evolution' of U history and oxygen isotope exchange in PRs. The igneous rocks clustered at the lower end of the curve, thus clearly distinguishing these PRs from the sedimentary ones. Old sedimentary PRs (Precambrian-Cambrian) with low $\delta^{18}O_p$ values also displayed lower U/P_2O_5 ratios. The younger sedimentary PRs (Cretaceous-Neogene), in turn, exhibited a wide range of U/P_2O_5 ratios with relatively high $\delta^{18}O_p$ values.

In igneous PRs, the low U concentration can be attributed to the lack of secondary U enrichment processes (Alschuler, 1958), whereas the low $\delta^{18}O_p$ values in PRs are likely due to a low concentration of ^{18}O in magmatic water and the limited oxygen isotopic fractionations in high temperature magmatic water (Taylor, 1968). In contrast, in sedimentary PRs, the time trend for U/P_2O_5 ratios and $\delta^{18}O_p$ values reflects a coincidence of paleoclimate and paleogeographic features. A low ratio in PRs indicates either that little U was further precipitated into francolite or that the U was released from the apatite lattices as a result of intensive post-depositional diagenetic processes. The latter process may also lower the $\delta^{18}O_p$ values (Shemesh et al., 1983). It is hard to find direct coupling of processes involved in U deposition and oxygen exchange, but findings rather indicate a time-dependent coincidence of processes altering U content and $\delta^{18}O_p$ signatures in a similar direction.

In summary, the results reported in this paper support the hypothesis that there is a co-evolution of $\delta^{18}O_p$ and U/P_2O_5 ratios in PRs across different geologic time units. Plotting both parameters against each other may provide a novel tool for PR dating, potentially supplementing existing dating tools, which are frequently valid for selected time windows only, in the case of Sr and U isotopes, for instance, precisely only for the 0-20 Ma and 0-1.2 Ma age range, respectively. On the other hand, the data clearly show that selecting mineral P fertilizers on the basis of the geological origin (igneous versus sedimentary) and age (Precambrian-Cambrian versus Cretaceous to Neogene) of their PRs may help to find $\delta^{18}O_p$ signatures of fertilizer P that differ from that of soil and plants and could thus be used as a tracer for elucidating the biological cycling of fertilizer P in the terrestrial environment (Tamburini et al., 2012; Amelung et al., 2015; Bauke et al., 2018).

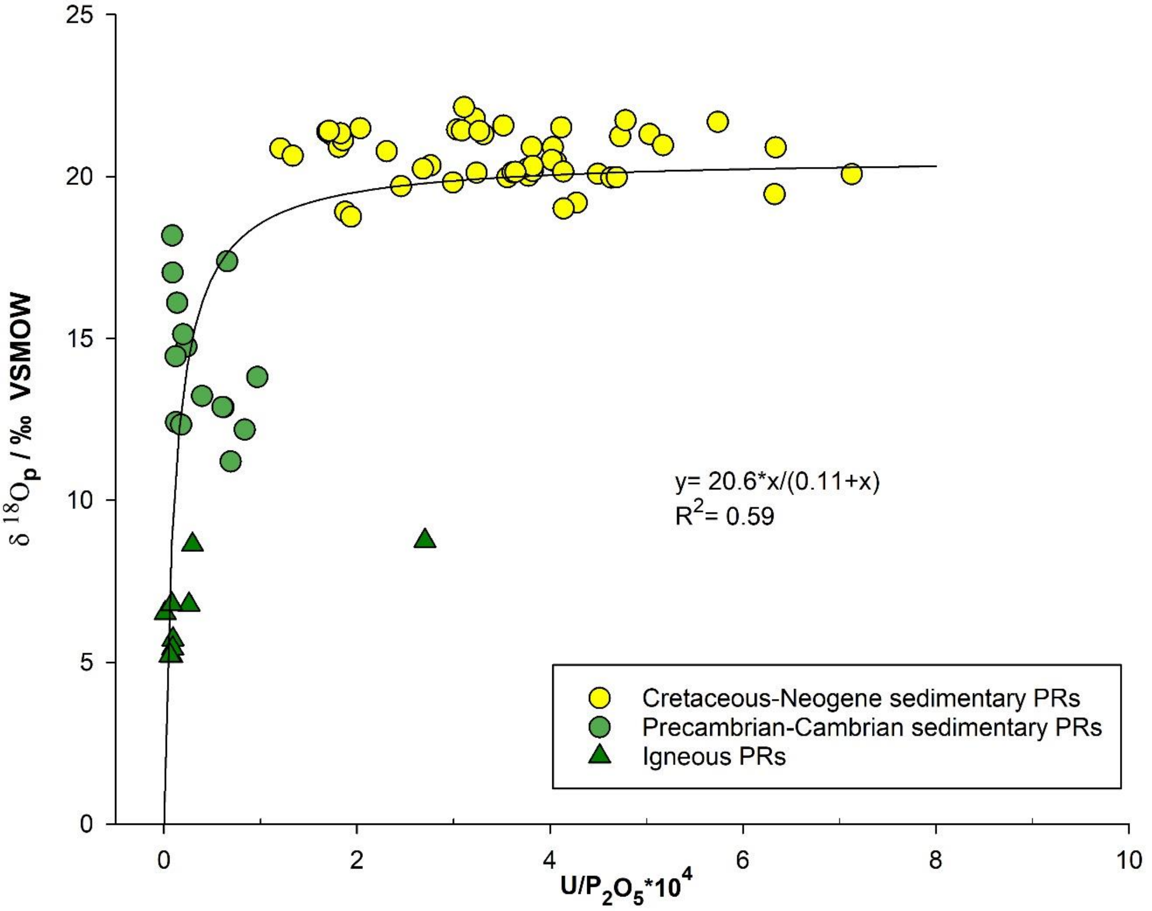

Figure 6. Correlation between oxygen isotope composition of phosphate ($\delta^{18}O_p$) and U/P_2O_5 in phosphate rocks (PRs).

4. Conclusion

To prevent and explain different levels of U contamination in agricultural soils, this work provides a comprehensive overview of U levels in various PRs worldwide and the underlining mechanisms of U accrual. We linked these data to information on the oxygen isotope composition of PRs, which provides additional information on the related genesis of P in these rocks. In soil, oxygen isotope abundance measurements of phosphates provide additional information on the efficiency of soil P cycling; yet, linking the latter to the origin of P fertilizers is still in its fledging stages (Tamburini et al., 2012; Amelung et al., 2015; Helfenstein et al., 2018).

The comprehensive overview of U levels in various PRs not only confirmed that igneous PRs contained lower levels of U than sedimentary PRs, but also that older sedimentary PRs (Precambrian-Cambrian) have less U than younger ones (Ordovician-Neogene). In addition, $\delta^{18}O_p$ distinguished the PRs deposits of: 1) igneous PRs ($\delta^{18}O_p$ = 5.2 to 8.8‰, e.g. from Russia), 2) old sedimentary PRs ($\delta^{18}O_p$ = 12.2 to 18.2‰, e.g. from China), and 3) younger sedimentary PRs ($\delta^{18}O_p$ = 18.8 to 22.1‰, e.g. from the USA). Finally, the differences of U levels in PRs were mirrored by the $\delta^{18}O_p$ signatures of the PRs, thus highlighting both their ‘co-evolution’, and inter changeability as a tracer of temporal or process changes in global PRs.

Acknowledgements

The authors would like to acknowledge the colleagues in Julius Kühn-Institut, Germany, for the help in collecting the phosphate rocks. They also express their sincere thanks to Dr. Tamburini and the colleagues in her group at ETH, and Dr. Bauke and Ye Wang at Bonn University, who helped establish and test the purification method for oxygen isotope analysis. We also want to Holger Wissel, in IBG-3, Forschungszentrum Jülich for performing the oxygen stable isotope analysis. This study was supported by the Chinese Scholarship Council (CSC201506350148).

References

Altschuler, Z. S., 1958. Geochemistry of uranium in apatite and phosphorite. US Geological Survey. 314-D: 45–90.

Altschuler, Z. S., 1980. The geochemistry of trace elements in marine phosphorites: Part I. Characteristic abundances and enrichment. The Society of Economic Paleontologists and Mineralogist Special Publication, 29: 19–30.

Amelung, W., Antar, P., Kleeberg, I., Oelmann, Y., Luecke, A., Alt, F., Lewandowski, H., Pätzold, S. and Barej, J., 2015. The $\delta^{18}O$ signatures of HCl-extractable soil phosphates: methodological challenges and evidence of the cycling of biological P in arable soil. European Journal of Soil Science, 66 (6): 965-972. https://doi.org/10.1111/ejss.12288

Avital, Y., Starinsky, A. and Kolodny, Y., 1983. Uranium geochemistry and fission-track mapping of phosphorites, Zefa field, Israel. Economic Geology, 78(1): 121-131. https://doi.org/10.2113/gsecongeo.78.1.121

Banerjee, D., Khan, M., Srivastava, N. and Saigal, G., 1982. Precambrian phosphorites in the Bijawar rocks of Hirapur-Bassia areas, sagar district, madhya pradesh, India. Mineralium Deposita, 17, 349-362. https://doi.org/10.1007/BF00204465

Baturin, G. and Kochenov, A., 2001. Uranium in phosphorites. Lithology and mineral resources, 36(4): 303-321. https://doi.org/10.1023/A:1010406103447

Bauke, S.L., von Sperber, C., Tamburini, F., Gocke, M., Honermeier, B., Schweitzer, K., Baumecker, M., Don, A., Sandhage-Hofmann, A. and Amelung, W., 2018. Subsoil phosphorus is affected by fertilization regime in long-term agricultural experimental trials. European Journal of Soil Science, 69(1): 103-112. https://doi.org/10.1111/ejss.12516

Bigalke, M., Schwab, L., Rehmus, A., Tondo, P. and Flisch, M., 2018. Uranium in agricultural soils and drinking water wells on the Swiss Plateau. Environment Pollution. 233: 943-951. https://doi.org/10.1016/j.envpol.2017.09.06

Blake, R.E., Chang, S.J. and Lepland, A., 2010. Phosphate oxygen isotopic evidence for a temperate and biologically active Archaean ocean. Nature, 464(7291): 1029. https://doi.org/10.1038/nature08952

Brookfield, M., Hemmings, D. and Van Straaten, P., 2009. Paleoenvironments and origin of the sedimentary phosphorites of the Napo Formation (Late Cretaceous, Oriente Basin, Ecuador). Journal of South American Earth Sciences, 28(2): 180-192. https://doi.org/10.1016/j.jsames.2009.02.004

Burnett, W.C. and Veeh, H.H., 1977. Uranium-series disequilibrium studies in phosphorite nodules from the west coast of South America. Geochimica et Cosmochimica Acta, 41(6), pp.755-764.

Cevik, U., Baltas, H., Tabak, A. and Damla, N., 2010. Radiological and chemical assessment of phosphate rocks in some countries. Journal of hazardous materials, 182(1-3): 531-535. https://doi.org/10.1016/j.jhazmat.2010.06.064

Chase, C. G. and Perry, E. C., 1972. The oceans: growth and oxygen isotope evolution. Science, 177(4053), 992-994. https://doi.org/10.1126/science.177.4053.992

Chernoff, C.B. and Orris, G.J., 2002. Data set of world phosphate mines, deposits, and occurrences: Part A. geologic data; Part B. location and mineral economic data. 2002-156. https://doi.org/10.3133/ofr02156

Cook, P. J. 1972. Petrology and geochemistry of the phosphate deposits of northwest Queensland, Australia. Economic Geology, 67, 1193-1213. https://doi.org/10.2113/gsecongeo.67.8.1193

Cook, P., O'Brien, G., Burnett, W. and Riggs. S., 1990. Neogene to Holocene phosphorites of Australia. In: Burnett, W.C. and Riggs, S.R. (Eds). Phosphate Deposits of the World, Cambridge University Press, Cambridge, pp. 98-115.

Cook, P.J. and Shergold, J.H., 2005. Phosphate Deposits of the World: Volume 1: Proterozoic and Cambrian Phosphorites. Cambridge University Press.

Cook, P.J., 1984. Spatial and temporal controls on the formation of phosphate deposits- a review, Phosphate minerals. Springer, pp. 242-274. https://doi.org/10.1007/978-3-642-61736-2_7

Cuney, M., 2010. Evolution of uranium fractionation processes through time: driving the secular variation of uranium deposit types. Economic Geology, 105(3): 553-569. https://doi.org/10.2113/gsecongeo.105.3.553

Dar, S.A., Khan, K.F., Khan, S.A., Mir, A.R., Wani, H., Balaram, V., 2014. Uranium (U) concentration and its genetic significance in the phosphorites of the Paleoproterozoic Bijawar Group of the Lalitpur district, Uttar Pradesh, India.. Arabian Journal of Geosciences 7 (6), 2237–2248. doi.org/10.1007/s12517-013-0903-8.

Dissanayake, C. B. and Chandrajith, R., 2009. Phosphate mineral fertilizers, trace metals and human health. Journal of the National Science Foundation of Sri Lanka, 37(3): 153-165.

Dutton, A., Wilkinson, B. H., Welker, J. M., Bowen, G. J. and Lohmann, K. C., 2005. Spatial distribution and seasonal variation in $^{18}O/^{16}O$ of modern precipitation and river water across the conterminous USA. An International Journal, 19(20), 4121-4146. https://doi.org/ 10.1002/hyp.5876

Fayek, M., Horita, J. and Ripley, E.M., 2011. The oxygen isotopic composition of uranium minerals: A review. Ore Geology Reviews, 41(1):1-21. https://doi.org/10.1016/j.oregeorev.2011.06.005

Föllmi, K., 1996. The phosphorus cycle, phosphogenesis and marine phosphate-rich deposits. Earth-Science Reviews, 40(1-2): 55-124. https://doi.org/10.1016/0012-8252(95)00049-6

Hayumbu, P., Haselberger, N., Markowicz, A. and Valkovic, V., 1995. Analysis of rock phosphates by x-ray fluorescence spectrometry. Applied radiation and isotopes, 46(10): 1003-1005. https://doi.org/10.1016/0969-8043(95)00206-S

He, G., and Zhou, Y., 2015. Geology of Phosphate Rock in China: Distribution, Rock Type and Metallogenic Perspective. Global Environmental Research, 19, 91-96.

Helfenstein, J., Tamburini, F., von Sperber, C., Massey, M.S., Pistocchi, C., Chadwick, O.A., Vitousek, P.M., Kretzschmar, R. and Frossard, E., 2018. Combining spectroscopic and isotopic techniques gives a dynamic view of phosphorus cycling in soil. Nature communications, 9(1): 3226.

Hendricks, S. and Hill, W., 1950. The nature of bone and phosphate rock. Proceedings of the National Academy of Sciences, 36(12): 731-737. https://doi.org/10.1073/pnas.36.12.731

Holland, H.D., 1984. The chemical evolution of the atmosphere and oceans. Princeton University Press.

Howard, P. and M. Hough., 1979. On the geochemistry and origin of the D Tree, Wonarah, and Sherrin Creek phosphorite deposits of the Georgina Basin, northern Australia. Economic Geology, 74, 260-284. https://doi.org/10.2113/gsecongeo.74.2.260

Hren, M., Tice, M. and Chamberlain, C., 2009. Oxygen and hydrogen isotope evidence for a temperate climate 3.42 billion years ago. Nature, 462(7270): 205. https://doi.org/10.1038/nature08518

Jaffrés, J. B., Shields, G. A. and Wallmann, K., 2007. The oxygen isotope evolution of seawater: A critical review of a long-standing controversy and an improved geological water cycle model for the past 3.4 billion years. Earth-Science Reviews, 83(1-2), 83-122. https://doi.org/10.1016/j.earscirev.2007.04.002

Jaisi, D.P., Blake, R.E., 2014. Advances in using oxygen isotope ratios of phosphate to understand phosphorus cycling in the environment.. In: In Advances in Agronomy, 125. Academic Press, pp. 1–53.

Jallad, I. S., Abu Murry, O. S. and Sadaqah, R. M., 1989, Upper Cretaceous phosphorites of Jordan, in: Notholt, A. J. G, Sheldon R. P. and Davidson, D. F. (Eds.) Phosphate Deposit of the World, Vol. 2, Phosphate Rock Resources, Cambridge Univ. Press, pp. 344-351.

Jarvis, I., 1995. Phosphorite geochemistry: state-of-the-art and environmental concerns. Oceanographic Literature Review, 8: 639.

Kastner, M., Garrison, R., Kolodny, Y., Reimers, C. and Shemesh, A., 1990. Coupled changes of oxygen isotopes in PO_4^{3-} and CO_3^{2+} in apatite, with emphasis on the Monterey Formation, California. In: Riggs S.R., Burnett W.C. (Eds.), Phosphate Deposits of the World: Vol. 3, Genesis of Neogene to Modern Phosphorites, Cambridge Univ. Press, pp. 312-324

Klinkhammer, G.P. and Palmer, M.R., 1991. Uranium in the oceans: where it goes and why. Geochimica et Cosmochimica Acta, 55(7), pp.1799-1806.

Khater, A.E.M., Galmed, M.A., Nasr, M.M. and El-Taher, A., 2016. Uranium and rare earth elements in Hazm El-Jalamid phosphate, Saudi Arabia: concentrations and geochemical patterns comparison. Environmental Earth Sciences, 75, 1261. https://doi.org/10.1007/s12665-016-6063-x

Knauth, L. P. and Lowe, D. R., 2003. High Archean climatic temperature inferred from oxygen isotope geochemistry of cherts in the 3.5 Ga Swaziland Supergroup, South Africa. Geological Society of America Bulletin, 115(5), 566-580. https://doi.org/10.1130/0016-7606(2003)115<0566:HACTIF>2.0.CO;2

Knauth, L.P. and Epstein, S., 1976. Hydrogen and oxygen isotope ratios in nodular and bedded cherts. Geochimica et Cosmochimica Acta, 40(9): 1095-1108. https://doi.org/10.1016/0016-7037(76)90051-X

Kolodny, Y. and Luz, B., 1992. Isotope signatures in phosphate deposits: Formation and diagenetic history, Isotopic signatures and sedimentary records. In: Clauer N., Chaudhuri S. (Eds.), Lecture Notes in Earth Sciences, Springer, pp. 69-121.

Kolodny, Y., and Kaplan, I.R., 1970. Uranium isotopes in sea-floor phosphorites. Geochimica et Cosmochimica Acta, 34(1):3-24. https://doi.org/10.1016/0016-7037(70)90148-1

Kusakabe, M. and Matsubaya, O., 1986. Volatiles in Magmas, volcanic gases, and thermal waters. Bull. Volcanol. Soc. Japan Spec. Issue 30, 267-283 (in Japanese with English abstract).

Land, L. S. and Lynch, F. L. (1996). $\delta^{18}O$ values of mudrocks: more evidence for an ^{18}O-buffered ocean. Geochimica et Cosmochimica Acta, 60(17), 3347-3352. https://doi.org/10.1016/0016-7037(96)00185-8

Lecuyer, C., Grandjean, P. and Sheppard, S.M., 1999. Oxygen isotope exchange between dissolved phosphate and water at temperatures ≤ 135 °C: inorganic versus biological fractionations. Geochimica et Cosmochimica Acta, 63(6): 855-862. https://doi.org/10.1016/S0016-7037(99)00096-4

Levina, S.D., Smilkstyn, A.O. and Karpov, L.N., Radioactivity of Phosphorites, Litologiya fosforitonosnykh otlozhenii (Lithology of Phosphorite-Bearing Sediments), In: Sokolova, A.S. (Eds), Moscow: Nauka, 1976, pp. 148–155.

Longinelli, A. and Nuti, S., 1968. Oxygen-isotope ratios in phosphate from fossil marine organisms. Science, 160(3830): 879-882. https://doi.org/10.1126/science.160.3830.879

Longinelli, A. and Nuti, S., 1973. Revised phosphate-water isotopic temperature scale. Earth and Planetary Science Letters, 19(3): 373-376. https://doi.org/10.1016/0012-821X(73)90088-5

Lucas, J. and Abbas, M., 1989. Uranium in natural phosphorites: the Syrian example. L'uranium dans les phosphorites naturelles: l'exemple syrien. Sciences Géologiques, bulletins et mémoires, 42(3): 223-236. In: Lucas, J., Cook, J. P and Prevot, L. (Eds.), Sciences Géologiques. Bulletin, tome 42, n°3, pp. 223-236. https://doi.org/10.3406/sgeol.1989.1824

Makarov, E.A., 1963. Crystal chemistry of uranium minerals. In: Vinogradov, A.P. (Eds.), Basic Features of Uranium Behaviour. Moscow, AN SSSR, pp. 27-45 (in Russian).

McKelvey, V.E., 1967. Phosphate deposits, U.S. Geological Survey Bulletin, 1252-D, pp. 1-22.

McManus, J., Berelson, W.M., Klinkhammer, G.P., Hammond, D.E. and Holm, C., 2005. Authigenic uranium: relationship to oxygen penetration depth and organic carbon rain. Geochimica et Cosmochimica Acta, 69(1): 95-108.

Menzel, R.G., 1968. Uranium, radium, and thorium content in phosphate rocks and their possible radiation hazard. Journal of Agricultural and Food Chemistry, 16(2): 231-234.

Muehlenbachs, K., 1998. The oxygen isotopic composition of the oceans, sediments and the seafloor. Chemical Geology, 145(3): 263-273. https://doi.org/10.1016/S0009-2541(97)00147-2

Nathan, Y., 2012 Phosphate minerals. In: Nriagu JO, Moore PB (Eds.), Chapter 8, The Mineralogy and Geochemistry of Phosphorites. Springer Science & Business Media, ISBN: 978-3642617362

Notholt, A.J.G., 1986. Phosphate Deposits of the World: Volume 3, Neogene to Modern Phosphorites, 156. Cambridge University Press.

Obersteiner, M., Peñuelas, J., Ciais, P., Van Der Velde, M. and Janssens, I.A., 2013. The phosphorus trilemma. Nature Geoscience, 6(11): 897. https://doi.org/10.1038/ngeo1990

Pantelica, A., Salagean, M., Georgescu, I. and Pincovschi, E., 1997. INAA of some phosphates used in fertilizer industries. Journal of Radioanalytical and Nuclear Chemistry, 216(2): 261-264. https://doi.org/10.1007/BF02033788

Parker, H. 1984. Tennessee Valley Authority National Fertilizer Development Center progress 83 (No. TVA/OACD-84/4). Tennessee Valley Authority, Muscle Shoals, AL (USA). Office of Agricultural and Chemical Development.

Partin, C. A., Bekker, A., Planavsky, N. J., Scott, C. T., Gill, B. C., Li, C. and Love, G. D., 2013. Large-scale fluctuations in Precambrian atmospheric and oceanic oxygen levels from the record of U in shales. Earth and Planetary Science Letters, 2013, 369: 284-293. https://doi.org/10.1016/j.epsl.2013.03.031

Petr P., 2016. Phosphate Rocks, Apatites and their Synthetic Analogues - Synthesis, Structure, Properties and Applications, IntechOpen, https://doi.org/10.10.5772/62214.

Piper, D.Z. and Kolodny, Y., 1987. The stable isotopic composition of a phosphorite deposit: $\delta^{13}C$, $\delta^{34}S$, and $\delta^{18}O$. Deep Sea Research Part A. Oceanographic Research Papers, 34(5-6), pp.897-911. https://doi.org/10.1016/0198-0149(87)90044-6

Pokryshkin, V.I., 1981. Regularities of the Localization of Precambrian and Phanerozoic Commercial-Grade Phosphorite Deposits in the World, Moscow: Nedra.

Pufahl, P.K. and Groat, L.A., 2017. Sedimentary and Igneous Phosphate Deposits: Formation and Exploration: An Invited Paper. Economic Geology, 112(3): 483-516. https://doi.org/10.2113/econgeo.112.3.483

Robert, F. and Chaussidon, M., 2006. A palaeotemperature curve for the Precambrian oceans based on silicon isotopes in cherts. Nature, 443(7114): 969. https://doi.org/10.1038/nature05239

Rothbaum, H., McGaveston, D., Wall, T., Johnston, A. and Mattingly, G., 1979. Uranium accumulation in soils from long-continued applications of superphosphate. Journal of Soil Science, 30(1): 147-153. https://doi.org/10.1111/j.1365-2389.1979.tb00972.x

Sattouf, M., 2007. Identifying the origin of rock phosphates and phosphorous fertilizsers using isotope ratio techniques and heavy metal patterns. Landbauforschung Völkenrode Special Issue 311, Braunschweig.

Sattouf, M., Kratz, S., Diemer, K., Fleckenstein, J., Rienitz, D., Schiel, D. and Schnug, E., 2008. Significance of uranium and strontium isotope ratios for retracing the fate of uranium during the processing of phosphate fertilizers from rock phosphates. In: De Kok, L.J. and Schnug, E. (Eds). Loads and Fate of fertilizer-derived uranium. Backhuys Publishers, Leiden. pp: 978-90.

Sattouf, M., Kratz, S., Diemer, K., Rienitz, O., Fleckenstein, J., Schiel, D. and Schnug, E., 2007. Identifying the origin of rock phosphates and phosphorus fertilizers through high precision measurement of the strontium isotopes ^{87}Sr and ^{86}Sr. Landbauforschung Völkenrode, 57: 01-11.

Schnug, E. and Haneklaus, N., 2015. Uranium in phosphate fertilizers–review and outlook, In: Merkel B., Arab A. (Eds). Uranium-Past and Future Challenges. Springer, pp. 123-130. https://doi.org/10.1007/978-3-319-11059-2_14

Schnug, E., Haneklaus, S., Schnier, C. and Scholten, L., 1996. Issues of natural radioactivity in phosphates. Communications in Soil Science and Plant Analysis, 27(3-4): 829-841. https://doi.org/10.1080/00103629609369600

Shemesh, A., Kolodny, Y. and Luz, B., 1983. Oxygen isotope variations in phosphate of biogenic apatites, II. Phosphorite rocks. Earth and Planetary Science Letters, 64(3): 405-416. https://doi.org/10.1016/0012-821X(83)90101-2

Shemesh, A., Kolodny, Y. and Luz, B., 1988. Isotope geochemistry of oxygen and carbon in phosphate and carbonate of phosphorite francolite. Geochimica et Cosmochimica Acta, 52(11): 2565-2572. https://doi.org/10.1016/0016-7037(88)90027-0

Shepherd, T.J., Rankin, A.H. and Alderton, D.H., 1985. A practical guide to fluid inclusion studies. Blackie.

Sokolov, A. 1996. Evolution of the uranium potential of phosphorites. Geokhimiya, 1117-1119.

Soudry, D., Ehrlich, S., Yoffe, O. and Nathan, Y., 2002. Uranium oxidation state and related variations in geochemistry of phosphorites from the Negev (southern Israel). Chemical Geology, 189(3-4), pp.213-230.

Stephens, N.P. and Carroll, A.R., 1999. Salinity stratification in the Permian Phosphoria sea; a proposed paleoceanographic model. Geology, 27(10): 899-902. https://doi.org/10.1130/0091-7613(1999)027<0899:SSITPP>2.3.CO;2

Syers, J.K., Mackay, A.D., Brown, M.W. and Currie, L.D., 1986. Chemical and physical characteristics of phosphate rock materials of varying reactivity. Journal of the Science of Food and Agriculture, 37(11): 1057-1064. https://doi.org/10.1002/jsfa.2740371102

Tamburini, F., Bernasconi, S. M., Angert, A., Weiner, T. and Frossard, E. 2010. A method for the analysis of the δ18O of inorganic phosphate extracted from soils with HCl. European Journal of Soil Science, 61(6), 1025-1032. https://doi.org/10.1111/j.1365-2389.2010.01290.x

Tamburini, F., Pfahler, V., Bünemann, E.K., Guelland, K., Bernasconi, S.M. and Frossard, E., 2012. Oxygen isotopes unravel the role of microorganisms in phosphate cycling in soils. Environmental science & technology, 46(11): 5956-5962. https://doi.org/10.1021/es300311h

Tang, C., Shindo, S. and Machida, I., 1998. Topographical effects on the distributions of rainfall and ^{18}O distributions: a case in Miyake Island, Japan. Hydrological processes, 12(4), 673-682. https://doi.org/10.1002/(SICI)1099-1085(19980330)12:4<673::AID-HYP608>3.0.CO;2-Y

Taylor Jr, H. P. and Epstein, S., 1962. Relationship between ^{18}O/^{16}O ratios in coexisting minerals of igneous and metamorphic rocks: part 1: principles and experimental results. Geological Society of America Bulletin, 73(4), 461-480.https://doi.org/10.1130/0016-606(1962)73[461:RBORIC]2.0.CO;2

Taylor, H. P. 1968. The oxygen isotope geochemistry of igneous rocks. Contributions to mineralogy and Petrology, 19(1), 1-71. https://doi.org/10.1007/BF00371729

U.S. Geological Survey, 2018, Mineral commodity summaries 2018: U.S. Geological Survey, 200 p. https://doi.org/10.3133/70194932.

Van Kauwenbergh S. J., 2010. World phosphate rock reserves and resources. Muscle Shoals, IFDC.

Van Kauwenbergh, S. J., 1997. Cadmium and other minor elements in world resources of phosphate rock. Proceedings-Fertilizer Society No. 400, London.

Volkov, R., 1994. Geochemistry of uranium in Vendian-Cambrian phosphorites. Geokhimiya, 7, 1042-1051.

Wakefield, Z. T., 1980. Distribution of cadmium and selected heavy metals in phosphate fertilizer processing. National Fertilizer Development Center, Tennessee Valley Authority.

Windmann, H., 2019. A contribution to the risk assessment of uranium contamination in the food chain through phosphate containing fertilizers, feed and food additives. PhD thesis, Faculty of Life Science, Technical University of Braunschweig.

Zanin, Y. N., Zamirailova, A., Fomin, A., Gilinskaya, L. and Kireev, A., 2000. Uranium of sedimentary apatite in catagenesis. Geochemistry International, 38, 452-458. https://doi.org/10.1134/S001670290701003X

Zanin, Yu. N., Gilinskaya, L. G., Krasil'nikova, N. A., Krivoputskaya, L. M., Mirtov, Yu. V. and Stolpovskaya, V. N., 1985. Calcium phosphates in phosphates of different types. International Geology Review, 27(10): 1212-1229, https://doi.org/10.1080/00206818509466496

Supplementary material

‘Co-evolution’ of Uranium Concentration and Oxygen Stable Isotope in Phosphate Rocks

Y.Sun[1,2*], W. Amelung[1,2], B. Wu[1], S. Haneklaus[3], M. Maekawa[3], A. Lücke[1], E. Schnug[3], R. Bol[1]

[1]Institute of Bio- and Geosciences: Agrosphere (IBG-3), Forschungszentrum Jülich GmbH, 52425 Jülich, Germany

[2]University of Bonn, Institute of Crop Science and Resource Conservation, Soil Science and Soil Ecology, Nussallee 13, 53115 Bonn, Germany.

[3] Institute for Crop and Soil Science, Julius Kühn-Institut, Federal Research Institute for Cultivated Plants, Bundesallee 69, 38640 Braunschweig, Germany

* Corresponding author (yajie.sun@uni-bonn.de)

Table S1. Literature review and own data on uranium concentrations in phosphate rocks

Country	Deposit	Type	Age	U ppm	P_2O_5 %	U/P_2O_5	Reference
Algeria	Djebel Onk	Phosphatic limestone; pelletal; granular;	Late Paleocene	31.0	32.4	1.0	Cevik et al., 2010
Algeria	Djebel Onk	Phosphatic limestone; pelletal; granular;	Late Paleocene	25.0	28.0	0.9	Khater et al., 2016
Algeria	Djebel Kouif	-	-	100.0	27.9	3.6	Parker, 1984
Algeria	Gebel Onk	Granular	Paleocene	8-115, 60	22-30, 21	2.8	Pokryshkin,1981
Algeria	-	Rock phosphate	-	51.8	28.6	1.8	this study
Algeria	-	Rock phosphate	-	52.7	28.8	1.8	this study
Algeria	-	Rock phosphate	-	53.3	28.7	1.9	this study
Algeria	-	Rock phosphate	-	53.5	28.6	1.9	this study
Algeria	-	Calcined phosphate	-	59.9	31.1	1.9	this study
Algeria	-	Rock phosphate	Cretaceous-Eocene	45.0	25.9	1.7	this study
Algeria	-	Rock phosphate	-	47.8	29.7	1.6	this study
Algeria	-	Rock phosphate	-	48.6	30.0	1.6	this study
Algeria	Djebel Onk	Phosphatic limestone; pelletal; granular;	Late Paleocene	25.0	29.3	0.9	Van Kauwenbergh, 1997
Antarctica	Pensacola	Nodules, matrix	Devonian	260.0	30.0	8.6	Altschuler, 1980
Australia	Eastern slope	Nodules	Middle Miocene-Early Pliocene	27-303, 126	11.0	11.9	Cook et al., 1990
Australia	Eastern slope	Nodules	Middle Miocene-Early Pliocene	67.0	9.6	3-13,7.9	Cook et al., 1990
Australia	North Queensland	Argillite-type phosphorites	Early-Middle Cambrian	15-65, 48	7.8-39.1, 18.6	2.6	Cook, 1972
Australia	North Queensland	Replacement phosphorites	Early-Middle Cambrian	10-80, 43	28-39.2, 35.3	1.2	Cook, 1972

Australia	North Queensland	Pelletal phosphorites	Early-Middle Cambrian	45-130, 78	33.7-37.4, 35.6	2.2	Cook, 1972
Australia	Wonarah	Leached phosphorites	Early-Middle Cambrian	2-53, 21.9	17.3-30.9, 24.7	0.1-2.3, 0.9	Howard and Hough, 1979
Australia	D Tree	Leached	Early-Middle Cambrian	8-74, 23	14.4-27.9, 21.7	0.4-3.7,1.1	Howard and Hough, 1979
Australia	D Tree	Replacement phosphorites	Early-Middle Cambrian	18-45, 33	37.6-39.5, 38.7	0.5-1.2, 0.9	Howard and Hough, 1979
Australia	Sherrin Creek (Queensland)	Unleached phosphorites	Early-Middle Cambrian	5-42, 25	28-37.8, 25	0.6-4.3, 1.2	Howard and Hough, 1979
Australia	D Tree	Partly leached	Early-Middle Cambrian	19-86, 47	7.8-27.4, 19.9	1-5.2, 2.5	Howard and Hough, 1979
Australia	D Tree	Unleached phosphorites	Early-Middle Cambrian	19-61, 32	3.8-15.5, 8.6	3.1-5.6, 3.9	Howard and Hough, 1979
Australia	Duchess	-	Early Middle Cambrian	80.0	29.1	2.7	Parker, 1984
Australia	Duchess	-	Early Middle Cambrian	80.0	23.9	3.3	Parker, 1984
Australia	Duchess	-	Early Middle Cambrian	92.0	31.2	2.9	Van Kauwenbergh, 1997
Azeri	-	shelly	Ordovician	35-52, 43	5.7-14.4, 10	2.4-9.1, 5.6	Baturin and Kochenov, 2001
Brazil	Bambui	pelletal	Precambrian	30.0	19-35,27	1-1.5,1.2	Altschuler, 1980
Brazil	-	Rock phosphate	Middle-Late Proterozoic	38.1	28.6	1.3	this study
Brazil	-	Rock phosphate		67.5	25.0	2.7	this study
Burkina Faso	Kodjari	-	Middle-Late Proterozoic	125.0	25.4	4.9	Van Kauwenbergh, 1997
China	Wanjhawan	Vaguely granular	Early-Middle Cambrian	12.9	26.0	0.5	Volkov, 1994
China	Kunjan	Granular	Early-Middle Cambrian	15.8	31.0	0.5	Volkov, 1994
China	Undifferentiated	-	-	10.0	31.9	0.3	Parker, 1984
China	Undifferentiated	-	-	20.0	30.3	0.7	Parker, 1984
China	Hubei, Jingzhou	Sedimentary type	Late Proterozoic	2.0	22.2	0.1	this study

China	Hubei, Jingzhou	Sedimentary type	Late Proterozoic	2.6	30.7	0.1	this study
China	Hunan, Shimen	Metamorphic type	Late Proterozoic	3.0	25.0	0.1	this study
China	Hubei, Yichang	Sedimentary type	Late Proterozoic	3.0	22.2	0.2	this study
China	Hubei, Jingmen	Sedimentary type	Late Proterozoic	3.7	29.8	0.2	this study
China	Hubei, Yichang	Sedimentary type	Late Proterozoic	5.0	25.2	0.2	this study
China	Hubei, Yichang	Sedimentary type	Late Proterozoic	5.6	31.4	0.2	this study
China	Hubei, Yichang	Sedimentary type	Late Proterozoic	7.2	30.9	0.4	this study
China	Guizhou, Kaiyang	Sedimentary type	Late Proterozoic	11.4	28.9	0.7	this study
China	Sichuan, Shijiao	Sedimentary type	Middle-Late Devonian	19.5	29.8	0.5	this study
China	Yunnan, Kunming	Sedimentary type	Early Cambrian	14.7	23.8	0.6	this study
China	Sichuan, Hanyuan	Sedimentary type	Middle-Late Devonian	14.3	23.6	1.0	this study
China	Yunnan, Kunming	Sedimentary type	Early Cambrian	22.6	27.0	0.8	this study
China	Yunnan, Jinning	Sedimentary type	Early Cambrian	20.4	21.1	1.5	this study
China	Kaiyang	Sedimentary type	Late Proterozoic	31.0	35.9	0.9	Van Kauwenbergh, 1997
Egypt	East Sabaiya	-	Late Cretaceous	57.0	30.6	1.9	Cevik et al., 2010
Egypt	Kosseir	-		40.0	28.3	1.4	Parker, 1984
Egypt	Abu Tartur	Bedded	Late Cretaceous	40.0	26.5	1.5	Parker, 1984
Egypt	Safaga	Granular	Late Cretaceous	100.0	28.9	3.5	Parker, 1984
Egypt	Safaga	Bedded; pelletal;	Late Cretaceous	130.0	32.2	4.0	Parker, 1984
Egypt	Safaga	Bedded; pelletal;	Late Cretaceous	130.0	31.8	4.1	Parker, 1984
Egypt	Safaga	Granular	Late Cretaceous	70-120,95	25.0	3-5, 4	Sokolov, 1996

Egypt	Abu Tartur	Bedded	Late Cretaceous	120.0	31.7	3.8	Van Kauwenbergh, 1997
Egypt	West Makamid	-	-	100.0	26.5	3.8	Van Kauwenbergh, 1997
Egypt	Hamrawen	-	Late Cretaceous	110.0	22.2	5.0	Van Kauwenbergh, 1997
Estonia	Toolse	Shelly	Ordovician	15-45, 30	6.5-8.7,7.6	2.3-5.2, 3.7	Baturin and Kochenov, 2001
Estonia	Narva	Shelly	Ordovician	52-100, 76	6.4-7.1, 6.8	7.3-15.5, 9.4	Baturin and Kochenov, 2001
Estonia	Toolse	Shelly	Ordovician	34.0	11.5	2.9	Levina et al., 1976
Eygpt	El-Sibayia	Bedded	Late Cretaceous	89.0	30.0	3.0	Khater et al., 2016
Eygpt	El-Sibayia	Bedded	Late Cretaceous	89.0	27.0	3.3	Khater et al., 2016
India	Hirapur	stromatolitic	Proterozoic	3-120,			Banerjee et al., 1982
India	Uttar Pradesh	Granular	Proterozoic	1.7-129.7	28.8-31.8	0.05-4.23	Dar et al., 2014
India	Rajasthan	Stromatolitic	Early Proterozoic	20.0	40.1	0.5	Parker, 1984
India	Udaipur	stromatolitic	Proterozoic	30-100, 65	10-37, 23	2.8	Pokryshkin, 1981
India	Mussoorie	-	Early Cambrian	26.0	25.0	1.0	Van Kauwenbergh, 1997
India	Aravalli	Stromatolitic	Proterozoic	3.6-4.2, 4	31.7-33.1, 32.4	0.1	Zanin et al. 2000
India	Aravallian basin	Stromatolitic	Proterozoic	3.6	31.7	0.1	Zanin et al. 2000
India	Aravallian basin	Stromatolitic	Proterozoic	4.2	33.1	0.1	Zanin et al. 2000
Israel	Mishash	Granular	Late Cretaceous-Paleocene	105.0	22-33,27.5	3.3	Makarov, 1963
Israel	Arad	granular, pellets	Late Cretaceous	150.0	32.3	4.6	Parker, 1984
Israel	-	-	Paleogene	40-240,140	16-27,22	6.3	Pokryshkin, 1981
Israel	Oron	Granular	Late Cretaceous	8-115, 60	20-32, 26	2.3	Pokryshkin, 1981

Israel	Arad	granular, pellets	Late Cretaceous	153.0	32.1	4.8	Syers et al., 1986
Israel	Arad	Rock phosphate	Late Cretaceous	153.0	33.0	4.6	this study
Israel	Arad	Rock phosphate	Late Cretaceous	148.0	32.9	4.5	this study
Israel	-	Rock phosphate	-	128.0	33.9	3.8	this study
Israel	-	Rock phosphate	-	127.4	33.3	3.8	this study
Israel	-	Rock phosphate	-	125.0	33.1	3.8	this study
Israel	-	Rock phosphate	-	152.0	32.4	4.7	this study
Israel	-	Rock phosphate	-	111.0	26.8	4.1	this study
Israel	Oron	Granular	Late Cretaceous	99.0	33.6	2.9	Van Kauwenbergh, 1997
Israel	Arad	granular, pellets	Late Cretaceous	148.0	32.8	4.5	Van Kauwenbergh, 1997
Israel	Nahal Zin	Rock phosphate	Late Cretaceous	129.0	38.0	3.4	this study
Israel	Oron	Rock phosphate	Late Cretaceous	215.0	33.9	6.3	this study
Japan	submarine rise of the sea of Japan	Granular	Miocene	12-110, 50	10.5-32.3, 21.4	0.4-5,2.7	Baturin and Kochenov, 2001
Jordan	-	Granular	Late Cretaceous-Paleocene	67-155, 111	20-34, 27	4.1	Volkov, 1994
Jordan	El Hasa	Granular	Late Cretaceous Maastrichtian	82.0	32.5	2.5	Jallad et al., 1989
Jordan	El Hasa	Granular	Late Cretaceous Maastrichtian	105.0	33.9	3.1	Jallad et al., 1989
Jordan	-	Granular	Late Cretaceous-Paleocene	90-180,135	20-34,27	5.0	Nabil, 1992
Jordan	Ruseifa	Granular	Late Cretaceous	129.0	30.8	4.2	Parker, 1984

Jordan	El Hasa	Granular	Late Cretaceous Maastrichtian	8-180, 94	23-34,28	3.3	Pokryshkin, 1981
Jordan	El Hasa	Granular	Late Cretaceous Maastrichtian	72.0	30.7	2.3	Syers et al., 1986
Jordan	Shidyia	granular	Late Cretaceous	46.0	30.5	1.5	Van Kauwenbergh, 1997
Jordan	El Hasa	Granular	Late Cretaceous	54.0	31.7	1.7	Van Kauwenbergh, 1997
Kazakhstan	Chilisai	Nodules	Eocene	16-53, 29	6.4-13.3, 9.8	2.9	Levina et al., 1976
Kazakhstan	Kara Tau	Bedded (microcrystalline)	Lower Cambrian	22.7	18.6	1.2	Zanin et al. 2000
Kazakhstan	Kara Tau	Bedded (microcrystalline)	Lower Cambrian	25.0	16.1	1.6	Zanin et al. 2000
Mali	Tilemsi	Nodules	Middle Eocene	123.0	28.8	4.3	Van Kauwenbergh, 1997
Mongolia	Hubsugul	Granular and structureless	Early Cambrian	1-31, 11	16-37, 20.7	0.5	Levina et al., 1976
Moricco	Ypussoufia	-	Late Cretaceous-Early Eocene	83.0	30.0	2.8	Cevik et al., 2010
Morocco	-	Granular	Late Cretaceous-Eocene	140.0	33.0	4.2	Altschuler, 1980
Morocco	-	-	-	140.0	33.0	4.2	Altschuler, 1980
Morocco	Khouribge	Bedded	Late Cretaceous-Early Eocene	88.0	33.0	2.7	Khater et al., 2016
Morocco	Youssoufia	Bedded	Late Cretaceous-Early Eocene	97.0	31.0	3.1	Khater et al., 2016
Morocco	Bu Craa	Bedded	Late Cretaceous-Paleocene	70.0	35.3	2.0	Parker, 1984
Morocco	Bu Craa	Bedded	Late Cretaceous-Paleocene	80.0	34.9	2.3	Parker, 1984

Morocco	-	-	-	120.0	31.8	3.8	Parker, 1984
Morocco	-	-	-	130.0	32.2	4.0	Parker, 1984
Morocco	-	Granular	Late Cretaceous-Eocene	57-190, 120	15-33, 24	5.0	Pokryshkin, 1981
Morocco	-	Rock phosphate	-	112.0	31.0	3.6	this study
Morocco	-	Rock phosphate	-	191.0	30.2	6.3	this study
Morocco	-	Rock phosphate	-	127.4	30.8	4.1	this study
Morocco	-	Rock phosphate	-	147.0	34.4	4.3	this study
Morocco	Khouribga	Rock phosphate	Late Cretaceous-Middle Eocene	127.5	31.4	4.1	this study
Morocco	Khouribga	Rock phosphate	Late Cretaceous-Middle Eocene	128.0	31.9	4.0	this study
Morocco	Khouribga	Rock phosphate	Late Cretaceous-Middle Eocene	245.0	34.4	7.1	this study
Morocco	Khouribga	Bedded; granular; shell	Late Cretaceous-Middle Eocene	81.0	32.3	2.5	Van Kauwenbergh, 1997
Morocco	Khouribga	Bedded; granular; shell	Late Cretaceous-Middle Eocene	100.0	33.4	3.0	Van Kauwenbergh, 1997
Morocco	Youssoufia	Bedded	Late Cretaceous-Early Eocene	111.0	32.5	3.4	Van Kauwenbergh, 1997
Morocco	Khouribga	Bedded; granular; shell	Late Cretaceous-Middle Eocene	82.0	33.4	2.5	Van Kauwenbergh, 1997
Morocco	Youssoufia	Bedded	Late Cretaceous-Early Eocene	97.0	32.1	3.0	Van Kauwenbergh, 1997

Morocco	Youssoufia	Bedded	Late Cretaceous-Early Eocene	89.0	27.6	3.2	Van Kauwenbergh, 1997
Nauru	-	-	-	40.0	37.1	1.1	Parker, 1984
Nauru	-	-	-	50.0	38.5	1.3	Parker, 1984
Nauru	-	-	-	60.0	38.7	1.6	Parker, 1984
Nauru	-	-	-	64.0	35.7	1.8	Syers et al., 1986
New zealand	submarine bChatham rise	Granular	Miocene	117-524, 230	21.8	5-24,14	Kolodny and Kaplan, 1970
Niger	Tapoa	Granular	Early Cambrian	7.1	27.0	0.3	Volkov, 1994
Niger	Tapoa	Granular	Late Proterozoic	8.2	31.0	0.3	Volkov, 1994
Niger	Parc W	-		65.0	33.5	1.9	Van Kauwenbergh, 1997
Peru	Peru shelf	Curst	Pleistocene-Holocene	12-38, 23	2.1-9.4, 4.4	3-8.3,5	Baturin and Kochenov, 2001
Peru	Peru shelf	Curst	Pleistocene-Holocene	52-193, 106	11.2-25.2, 14.7	4.6-8.3,4.9	Baturin and Kochenov, 2001
Peru	Peru shelf	Nodular	Pleistocene-Holocene	16-182, 93	5.9-28.7, 17.3	2.0-17.7,5.3	Burnett and Veeh,1977
Peru	Sechura	Pelletal	Middle Miocene	72.0	29.5	2.4	Parker, 1984
Peru	Sechura	Pelletal	Middle Miocene	80.0	30.8	2.6	Parker, 1984
Peru	Sechura	Pelletal	Middle Miocene	80.0	29.7	2.7	Parker, 1984
Peru	Sechura	Pelletal	Middle Miocene	47.0	29.3	1.6	Van Kauwenbergh, 1997
Peru	Sechura	Pelletal	Middle Miocene	80.0	31.3	2.6	Van Kauwenbergh, 1997
Portugal	Continental slope	Nodular	Miocene	5-158, 80	6.4-21.5, 14	0.5-11.1,5.5	Gaspar, 1981
Russia	Seleuk	Nodules	Late Jurassic-Paleogene	4.2	13.5	0.3	Baturin and Kochenov, 2001
Russia	Egor'ev	Nodular	Late Jurassic-early Cretaceous	17.0	12.6	1.3	Baturin and Kochenov, 2001

Russia	Penze	Nodules	Late Jurassic-Paleogene	31.0	24.1	1.3	Baturin and Kochenov, 2001
Russia	Bessonov	Nodules	Late Jurassic-Paleogene	27.0	19.2	1.4	Baturin and Kochenov, 2001
Russia	Bogdanov	Nodules	Late Jurassic-Paleogene	27.0	18.4	1.5	Baturin and Kochenov, 2001
Russia	Trukhanov	Nodules	Late Jurassic-Paleogene	27.0	17.9	1.5	Baturin and Kochenov, 2001
Russia	Tarkhanov	Nodules	Late Jurassic-Paleogene	31.0	20.1	1.5	Baturin and Kochenov, 2001
Russia	Tambov	Nodules	Late Jurassic-Paleogene	45.0	24.9	1.8	Baturin and Kochenov, 2001
Russia	Kingisepp, Baltic region	Shelly	Ordovician	24.0	12.5	2.0	Baturin and Kochenov, 2001
Russia	Egor'ev	Nodular	Late Jurassic-early Cretaceous	50.0	23.3	2.1	Baturin and Kochenov, 2001
Russia	Podbuga	Nodules	Late Jurassic-Paleogene	45.0	18.3	2.5	Baturin and Kochenov, 2001
Russia	Krolevitskoe	Nodules	Late Jurassic-Paleogene	40.0	16.1	2.5	Baturin and Kochenov, 2001
Russia	Undor	Nodules	Late Jurassic-Paleogene	59.0	23.2	2.5	Baturin and Kochenov, 2001
Russia	Oraush	Nodules	Late Jurassic-Paleogene	68.0	25.3	2.7	Baturin and Kochenov, 2001
Russia	Polpino	Nodules	Late Cretaceous	52.0	16.1	3.2	Baturin and Kochenov, 2001
Russia	Shchigrov	Nodules	Late Jurassic-Paleogene	68.0	16.0	4.3	Baturin and Kochenov, 2001
Russia	Slobodsk-Kostoretsk	Nodules	Late Jurassic-Paleogene	40.0	6.9	5.8	Baturin and Kochenov, 2001
Russia	Trekhostrovsk	Nodules	Late Jurassic-Paleogene	88.5	12.6	7.0	Baturin and Kochenov, 2001
Russia	Vyatka-Kama	Nodules	Late Jurassic-Paleogene	17-59, 38	12.6-23.3, 18.0	0.7-4.6, 2.6	Baturin and Kochenov, 2001
Russia	Maardu, ibidem	Shelly	Ordovician	14-68, 41	10.8-26, 18	1.3-2.6, 2.0	Baturin and Kochenov, 2001
Russia	Maardu, ibidem	Shelly conglomerate	Ordovician	24.0	17.0	1.4	Levina et al., 1976

Russia	Maardu, ibidem	shelly	Ordovician	7-48, 21	3.0-29, 13	1.6	Levina et al., 1976
Russia	Egor'ev	Nodular	Late Jurassic-early Cretaceous	34.0	21.1	1.6	Levina et al., 1976
Russia	Egor'ev	Phosphatized fauna	Late Jurassic-early Cretaceous	40.0	32.1	1.7	Levina et al., 1976
Russia	Vyatka-Kama	Phosphatized fauna	Late Jurassic-Paleogene	40.0	23.1	1.7	Levina et al., 1976
Russia	Gornaya shoria	Brecciated	Late Proterozoic	10-60, 35	5-13.6, 12	2.4	Levina et al., 1976
Russia	Maardu, ibidem	Phosphatized sandstone	Ordovician	20.0	8.2	2.4	Levina et al., 1976
Russia	Lagap(Shantar Island)	Brecciated	Early-Middle Cambrian	7-56, 25	5-32, 20	2.5	Levina et al., 1976
Russia	Vyatka-Kama	Nodules	Late Jurassic-Paleogene	17-58, 34	10.7-19.5, 12.2	2.8	Levina et al., 1976
Russia	Maardu, ibidem	Pebble	Ordovician	25.0	8.6	2.9	Levina et al., 1976
Russia	Polpino	Nodules	Late Cretaceous	1-111, 43	5-8, 7	2-12, 4.8	Levina et al., 1976
Russia	Polpinsk	Nodular	Upper Cretaceous	30.4	27.8	1.1	Zanin et al. 2000
Russia	Egor'ev	Nodular	Upper Jurassic-lower Cretaceous	29.6	25.8	1.1	Zanin et al. 2000
Russia	Egor'ev	Nodular	Upper Jurassic-lower Cretaceous	29.6	25.8	1.1	Zanin et al. 2000
Russia	Egor'ev	Nodular	Upper Jurassic-lower Cretaceous	30.7	25.5	1.2	Zanin et al. 2000
Russia	Polpinsk	phosphatic wood	Upper Cretaceous	55.8	28.5	2.0	Zanin et al. 2000
Russia	Egor'ev	Nodular	Upper Jurassic-lower Cretaceous	35.2	15.8	2.2	Zanin et al. 2000
Russia	Polpinsk	phosphatic wood	Upper Cretaceous	66.5	28.8	2.3	Zanin et al. 2000

Russia	Polpinsk	phosphatic wood	Upper Cretaceous	100.0	20.8	4.8	Zanin et al. 2000
Russia	Sakhalin Island	Nodular	Neogene	8.2	15.5	0.5	Zanin et al. 2000
Russia	Sakhalin Island	Nodular	Neogene	17.9	26.8	0.7	Zanin et al. 2000
Saudi Arabia	Al-Jalamid	bedded; pelletal	Early Paleocene	21.0	21.0	1.0	Khater et al., 2016
Saudi Arabia	Al-Jalamid	bedded; pelletal	Early Paleocene	21.0	21.0	1.0	Khater et al., 2016
Saudi Arabia	Amm Wa ual	bedded; pelletal	Paleocene-Oligocene	61.0	32.0	1.9	Khater et al., 2016
Saudi Arabia	Amm Wa ual	bedded; pelletal	Paleocene-Oligocene	62.0	27.0	2.3	Khater et al., 2016
Saudi arabia	-	Granular	Late Cretaceous-Paleocene	16-90, 53	18.1-31.4, 24.7	2.1	Pokryshkin, 1981
Seamounts of the Pacific Ocean	-	Phosphatized limestones, breccia, and effusives	Late Cretaceous-Quaternary	1.3-9.2	4.8-31.6	0.06-0.7	Baturin et al., 1982
Senegal	Taiba	Bedded	Middle Eocene-Oligocene	67.0	36.0	1.9	Khater et al., 2016
Senegal	Taiba	Rock phosphate	Middle Eocene-Oligocene	96.0	36.7	2.6	this study
Senegal	Taiba	Rock phosphate	Middle Eocene-Oligocene	90.0	36.6	2.5	this study
Senegal	Taiba	Granular	Middle Eocene-Oligocene	70.0	27.2	2.6	Parker, 1984
Senegal	Taiba	Granular	Middle Eocene-Oligocene	100-150,125	25-31, 29	2.6	Pokryshkin, 1981
Senegal	Taiba	Granular	Middle Eocene-Oligocene	64.0	36.9	1.7	Van Kauwenbergh, 1997
Senegal	Taiba	Granular	Middle Eocene-Oligocene	99.0	37.0	2.6	Zanin et al. 2000
Senegal	Taiba	Granular	Middle Eocene-Oligocene	154.0	38.0	4.1	Zanin et al. 2000
Siberia	Siberian platform, Vikhoreva river	Shelly	Middle Ordovician	11.0	38.2	0.3	Zanin et al. 2000

	area, Angara River Basin						
Siberia	Siberian platform, Vikhoreva river area, Angara River Basin	Shelly	Middle Ordovician	11.0	37.2	0.3	Zanin et al. 2000
Siberia	Siberian platform, Kuonamka Formation, Kachelkuan River valley	Nodular	Upper Lower Cambrain	56.6	29.0	2.0	Zanin et al. 2000
Siberia	Siberian platform, Kuonamka Formation, Kachelkuan River valley	Nodular	Upper Lower Cambrain	374.2	26.1	14.3	Zanin et al. 2000
South Africa				11.2	38.0	0.3	this study
Southern of African	Agulhas Bank	Nodular	Miocene-Pliocene	10-166, 79	17.3-24, 21	0.4-9.8, 5.1	Kolodny and Kaplan, 1970
Syria	-	Granular	Late Cretaceous-Paleocene	120-140, 130	25.0	4-6, 5	Volkov, 1994
Syria	-	Granular	Late Cretaceous-Paleocene	30-200,115	25.0	4.6	Baturin and Kochenov, 2001
Syria	Hims-Palmyra (Alsharqia)	-	Late Cretaceous	36.0	26.7	1.4	Cevik et al., 2010
Syria	-	Granular	Late Cretaceous-Paleocene	20-319, 82	18-36, 26.3	3.2	Lucas and Abbas, 1989
Syria	-	Rock phosphate	-	58.6	24.6	2.4	this study
Syria	-	Rock phosphate	-	58.6	24.6	2.4	this study
Syria	Khneifies	bedded	Late Cretaceous	75.0	31.9	2.4	Van Kauwenbergh, 1997
Syria	Khnefies	Ground rock phosphate	Late Cretaceous	59.5	30.4	2.0	this study

Syria	Ain Layloun	Friable phosphate rock	Cretaceous	137.6	31.2	4.4	this study
Tanzania	Minjingu	-	Neogene-Quaternary	390.0	28.6	13.6	Van Kauwenbergh, 1997
Togo	-		Middle Eocene	110.0	36.7	3.0	Parker, 1984
Togo	-	Rock phosphate		107.0	36.4	2.9	this study
Togo	-	Rock phosphate	Early-Middle Eocene	104.0	33.7	3.1	this study
Togo	-	Rock phosphate	-	96.7	36.0	2.7	this study
Togo	-	-	-	77.0	36.5	2.1	Van Kauwenbergh, 1997
Togo	-	-	Early-Middle Eocene	93.0	37.0	2.5	Khater et al., 2016
Tunisia	Gafsa	-	Paleocene-Early Eocene	20.0	26.1	0.8	Cevik et al., 2010
Tunisia	-	-		44.0	29.0	1.5	Khater et al., 2016
Tunisia	-	-	Paleocene-Early Eocene	12.0	29.2	0.4	Parker, 1984
Tunisia	-	-	Paleocene-Early Eocene	30.0	29.5	1.0	Parker, 1984
Tunisia	-	-	Paleocene-Early Eocene	40.0	29.2	1.4	Parker, 1984
Tunisia	-	-	Paleocene-Early Eocene	50.0	28.0	1.8	Parker, 1984
Tunisia	-	-	Paleocene-Early Eocene	88.0	30.7	2.9	Parker, 1984
Tunisia	Gafsa	Granular	Paleogene	35-75, 55	25-31, 28	2.3	Pokryshkin, 1981
Turkey	Mardin	Granular	Late Cretaceous-Paleocene	25-57, 40	10-25, 17.5	2.3	Baturin and Kochenov, 2001
Turkey	Mazidagi	bedded; pelletal; nodular; oolitic; fossiliferous (fish remains and bones); limonitic and glauconitic phosphatic limestone	Late Cretaceous	33.0	33.5	1.0	Cevik et al., 2010
Ukraine	Podol region	Concretionary radiated	Vendian	0.6	24.8	0.0	Zanin et al. 2000

Ukraine	Podol region	Concretionary radiated	Vendian	0.9	35.3	0.0	Zanin et al. 2000
Ukraine	Podol region	Concretionary radiated	Vendian	3.4	33.0	0.1	Zanin et al. 2000
Ukraine	Podol region	Concretionary radiated	Vendian	4.2	35.1	0.1	Zanin et al. 2000
USA	Continental slope of Carolina	Nodular	Miocene	40-130, 77	22.4-29.7, 26	1.4-5.8,3.6	Altschuler et al., 1958
USA	Pango River, North Carolina	Granular	Miocene	65.0	30.0	2.0	Altschuler, 1980
USA	Bone Valley, Florida	Granular and nodular	Miocene-Pliocene	140.0	30-35, 33	4.4	Altschuler, 1980
USA	Phosphoria	Microgranular	Permian	20-210, 90	23-37, 30	3.0	Gulbrandsen, 1966
USA	North Florida	-		81.0	31.0	2.6	Khater et al., 2016
USA	Idaho	-	Middle-Late Permian	107.0	32.0	3.3	Khater et al., 2016
USA	Florida	-	Early-Middle Miocene	141.0	32.0	4.4	Khater et al., 2016
USA	submarine blake plateau	Nodular	Miocene	18-70, 37	18-20, 19	1-4,2.5	Kolodny and Kaplan, 1970
USA	North Florida	-	Miocene-Pliocene	50.0	30.9	1.6	Parker, 1984
USA	North Carolina	bedded; granular	Early-Middle Miocene	60.0	30.5	2.0	Parker, 1984
USA	North Florida	-	Miocene-Pliocene	70.0	32.5	2.2	Parker, 1984
USA	Idaho	peloidal	Middle-Late Permian (late paleozoic)	70.0	32.3	2.2	Parker, 1984
USA	North Carolina	bedded; granular	Early-Middle Miocene	70.0	30.0	2.3	Parker, 1984
USA	North Carolina	bedded; granular	Early-Middle Miocene	93.0	30.2	3.1	Parker, 1984
USA	Idaho	peloidal	Middle-Late Permian (late paleozoic)	110.0	32.0	3.4	Parker, 1984

USA	Idaho	peloidal	Middle-Late Permian (late paleozoic)	110.0	30.2	3.6	Parker, 1984
USA	Central Florida	-	Neogene	120.0	32.2	3.7	Parker, 1984
USA	Central Florida	-	Neogene	160.0	32.7	4.9	Parker, 1984
USA	Central Florida	-	Neogene	150.0	27.8	5.4	Parker, 1984
USA	Central Florida	-	Neogene	200.0	30.7	6.5	Parker, 1984
USA	lower Carolina	Nodular	Neogene	3-65, 30	8.5-21, 15	2.0	Pokryshkin, 1981
USA	Hawthorne Formation, Florida	Granular and nodular	Miocene	40-65, 50	10-25, 17	3.0	Pokryshkin, 1981
USA	North Carolina	Granular	Miocene	25-250, 135	11-18, 15	9.0	Pokryshkin, 1981
USA	North Carolina	bedded; granular	Early-Middle Miocene	65.0	29.1	2.2	Syers et al., 1986
USA	North Florida	-	Miocene-Pliocene	143.0	30.5	4.7	Syers et al., 1986
USA	Florida	Rock phosphate	-	74.0	32.1	2.3	this study
USA	North Florida	Pebble phosphate	-	103.0	31.1	3.3	this study
USA	North Florida	Rock phosphate	Early-Middle Miocene; Holocene	104.0	33.5	3.1	this study
USA	South Florida	Pebble phosphate	-	128.0	36.0	3.6	this study
USA	Florida	Pebble phosphate	-	114.0	32.4	3.5	this study
USA	Florida	Pebble phosphate	-	112.0	34.3	3.3	this study
USA	Florida	Rock phosphate	late Miocene	95.3	31.4	3.0	this study
USA	Florida	Rohphosphat normal (Pebble-Phosphat)	Early-Middle Miocene	154.0	32.6	4.7	this study
USA		Pebble phosphate, commercial quality	-	153.0	30.4	5.0	this study
USA		Pebble phosphate	-	104.2	32.4	3.2	this study

USA	Florida	Rohphosphat Pebble	Early-Middle Miocene	147.0	28.4	5.2	this study
USA	Florida	Rock phosphate (as raw material)	Early-Middle Miocene	191.0	33.3	5.7	this study
USA	Central Florida	-	Neogene	128.4	34.6	3.7	Van Kauwenbergh, 1997
USA	Idaho	peloidal	Middle-Late Permian (late paleozoic)	141.0	30.2	4.7	Van Kauwenbergh, 1997
USA	Central Florida	-	Neogene	135.0	33.3	4.0	Van Kauwenbergh, 1997
USA	North Carolina	bedded; granular	Early-Middle Miocene	41.0	29.9	1.4	Van Kauwenbergh, 1997
USA	Idaho	peloidal	Middle-Late Permian (late paleozoic)	60.0	32.6	1.8	Van Kauwenbergh, 1997
USA	Central Florida	-	Neogene	59.0	31.0	1.9	Van Kauwenbergh, 1997
USA	North Carolina	bedded; granular	Early-Middle Miocene	70.0	32.2	2.2	Van Kauwenbergh, 1997
USA	Central Florida	-	Neogene	128.5	34.5	3.7	Van Kauwenbergh, 1997
USA	North Carolina	bedded; granular	Early-Middle Miocene	58.0	28.1	2.1	Wakefield, 1980
USA	North Florida	-	Miocene-Pliocene	69.0	32.7	2.1	Wakefield, 1980
USA	North Florida	-	Miocene-Pliocene	66.0	31.1	2.1	Wakefield, 1980
USA	North Carolina	bedded; granular	Early-Middle Miocene	69.0	29.9	2.3	Wakefield, 1980
USA	North Carolina	bedded; granular	Early-Middle Miocene	62.0	26.2	2.4	Wakefield, 1980
USA	North Florida	-	Miocene-Pliocene	86.0	28.1	3.1	Wakefield, 1980
USA	Idaho	peloidal	Middle-Late Permian (late paleozoic)	135.0	32.7	4.1	Wakefield, 1980
USA	Central Florida	-	Neogene	140.0	33.3	4.2	Wakefield, 1980

USA	Central Florida	-	Neogene	140.0	33.0	4.2	Wakefield, 1980
USA	Idaho	peloidal	Middle-Late Permian (late paleozoic)	138.0	31.3	4.4	Wakefield, 1980
USA	Central Florida	-	Neogene	152.0	32.5	4.7	Wakefield, 1980
USA	Central Florida	-	Neogene	156.0	30.1	5.2	Wakefield, 1980
USA	Central Florida	-	Neogene	166.0	30.5	5.4	Wakefield, 1980
USA	Kentucky	Nodular	Upper Devonian-Lower Carboniferous	20.6	23.4	0.9	Zanin et al. 2000
USA	Kentucky	Nodular	Upper Devonian-Lower Carboniferous	53.4	23.6	2.3	Zanin et al. 2000
USA	phosphoria formation	Bedded (microcrystalline)	Upper Permian	41.7	13.0	3.2	Zanin et al. 2000
USA	phosphoria formation	Bedded (microcrystalline)	Upper Permian	108.5	33.8	3.2	Zanin et al. 2000
USA	phosphoria formation	Bedded (microcrystalline)	Upper Permian	123.1	23.2	5.3	Zanin et al. 2000
USA	phosphoria formation	Bedded (microcrystalline)	Upper Permian	194.0	34.2	5.7	Zanin et al. 2000
Venezuela		-	Late Cretaceous-Paleogene	65-80, 72	27.9	3.5	Volkov, 1994
Venezuela	Recieto	-	-	51.0	15-35.6, 25.3	1.8	Van Kauwenbergh, 1997
Western Sahara	Bu Craa	Granular	Paleocene	40-90, 65	37.0	2.6	Pokryshkin, 1981
Russia	Kola	Igneous type	-	6.0			Menzel, 1968
Finland	-	Igneous type	-	0.2			Schnug et al., 1996
Russia	Kola	Igneous type	-	3.0			Schnug et al., 1996
South Africa		Igneous type	-	10.0			Schnug et al., 1996

South Africa		Igneous type	-	23.0			schnug, 2007
Brazil	Araxa	Igneous type	-	117.0	37.0	3.2	Syers et al., 1986
Brazil	-	Igneous type	-	59.2	15.5	3.8	this study
Brazil	-	Igneous type	-	18.7	27.0	0.7	this study
China	Hebei	Igneous type	-	0.3	29.1	0.0	this study
China	Hunan	Igneous type	-	2.7	33.9	0.1	this study
Finland	-	Igneous type	-	0.9	49.1	0.0	this study
Russia	Kola	Igneous type	-	3.2	40.1	0.1	this study
Russia	Kola	Igneous type	-	3.7	40.0	0.1	this study
Russia	Kola	Igneous type	-	3.5	38.6	0.1	this study
Russia	Kola	Igneous type	-	2.5	39.0	0.1	this study
Russia	Kola	Igneous type	-	27.0	36.0	0.8	this study
Brazil	Araxa	Igneous type	-	247.0	37.4	6.7	Van Kauwenbergh, 1997
Brazil	Catalao	Igneous type	-	220.0	33.3	5.9	Van Kauwenbergh, 1997
Finland	Siilinjarvi	Igneous type	-	37.0	39.5	0.9	Van Kauwenbergh, 1997
Russia	Kola	Igneous type	-	20.0	38.1	0.5	Van Kauwenbergh, 1997
Russia	Kola	Igneous type	-	20.0	40.1	0.5	Van Kauwenbergh, 1997
Russia	Kola	Igneous type	-	30.0	22.9	1.3	Van Kauwenbergh, 1997
Russia	Kola	Igneous type	-	40.0	32.4	1.2	Van Kauwenbergh, 1997
South Africa	Phalaborwa	Igneous type	-	8.0	41.5	0.2	Van Kauwenbergh, 1997
South Africa	Phalaborwa	Igneous type	-	37.0	36.4	1.0	Van Kauwenbergh, 1997

Sweden	Kiiruna	Igneous type	-	20.0			Van Kauwenbergh, 1997
Zimbabwe	Dorowa	Igneous type	-	8.0	33.1	0.2	Van Kauwenbergh, 1997

Table S2. $\delta^{18}O_p$ in sedimentary phosphate rocks of different geological ages in this study.

Country	Deposit	Age	Estimated age (Million years)	$\delta^{18}O_p$ (‰VSMOW)
Algeria	-	Cretaceous-Eocene	58	20.9
Algeria	-	Cretaceous-Eocene	58	21.1
Algeria	-	Cretaceous-Eocene	90	21.3
Algeria	-	Cretaceous-Eocene	58	21.3
Algeria	-	Cretaceous-Eocene	58	21.4
Algeria	-	Cretaceous-Eocene	58	21.4
Algeria	-	Cretaceous-Eocene	58	21.5
Brazil	-	-	-	11.2
Brazil	-	-	-	20.6
China	Yunnan, Kunming	Early Cambrian	535	12.2
China	Hubei, Yichang	Late Proterozoic	770	12.3
China	Hubei, Jingmen	Late Proterozoic	770	12.4
China	Yunnan, Kunming	Early Cambrian	535	12.9
China	Sichuan, Hanyuan	Middle-Late Devonian	376	12.9
China	Guizhou, Kaiyang	Late Proterozoic	770	13.2
China	Yunnan, Jinning	Early Cambrian	535	13.8
China	Hunan, Shimen	Late Proterozoic	770	14.5
China	Hubei, Yichang	Late Proterozoic	770	14.7
China	Hubei, Yichang	Late Proterozoic	770	15.1
China	Hubei, Yichang	Late Proterozoic	770	16.1
China	Hubei, Jingzhou	Late Proterozoic	770	17.0
China	Sichuan, Shijiao	Middle-Late Devonian	376	17.4
China	Hubei, Jingzhou	Late Proterozoic	770	18.2
Israel	-	Late Cretaceous	83	19.0
Israel	Arad	Late Cretaceous	83	20.0
Israel	-	Late Cretaceous	83	20.0
Israel		Late Cretaceous	83	20.0
Israel	Arad	Late Cretaceous	83	20.1
Israel	-	Late Cretaceous	83	20.2
Israel	-	Late Cretaceous	83	20.2
Israel	Nahal Zin	Late Cretaceous	83	20.3
Israel	Oron	Late Cretaceous	83	20.9
Israel	Nahal Zin	Late Cretaceous	83	20.9
Morocco	-	Late Cretaceous	72	19.2
Morocco	-	Late Cretaceous	72	19.5
Morocco	Khouribga	Late Cretaceous-Middle Eocene	72	20.1
Morocco	-	-	-	20.1

Morocco	-	-	-	20.1
Morocco	-	-	-	20.2
Morocco	Khouribga	Late Cretaceous-Middle Eocene	72	20.5
Morocco	Khouribga	Late Cretaceous-Middle Eocene	72	20.5
Senegal	Taiba	Middle Eocene-Oligocene	34	19.7
Senegal	Taiba	Middle Eocene-Oligocene	34	20.3
Syria	Khnefies	Late Cretaceous	83	18.8
Syria	Ain Layloun	Cretaceous	105	21.7
Togo	-	-	-	19.8
Togo	-	-	-	20.0
Togo	-	-	-	20.2
Togo	-	-	-	20.4
USA	-	-	-	20.1
USA	Florida	Miocene-Pliocene	13	20.8
USA	Florida	Miocene-Pliocene	13	21.0
USA	Florida	Miocene-Pliocene	13	21.2
USA	North Florida	-	13	21.3
USA	-	-	-	21.3
USA	Florida	Miocene-Pliocene	13	21.4
USA	South Florida		13	21.4
USA	Florida	Miocene-Pliocene	13	21.5
USA	Florida	Miocene-Pliocene	13	21.6
USA	Florida	Miocene-Pliocene	13	21.7
USA	-	-	-	21.8
USA	North Florida	Early-Middle Miocene; Holocene	0.01	22.1

Table S3. $\delta^{18}O_p$ in igneous phosphate rocks from different deposits in this study.

Deposit	**$\delta^{18}O_p$ (‰VSMOW)**
Brazil	8.8
Hebei, China	6.5
Hebei, China	6.8
Liaoning, China	6.8
South Africa	8.6
Kola, Russia	5.2
Kola, Russia	5.7
Kola, Russia	5.4
Kola, Russia	5.2